



Office de la Propriété

Intellectuelle
du Canada

Un organisme
d'Industrie Canada

Canadian
Intellectual Property
Office

An agency of
Industry Canada

CA 2378184 C 2009/05/26

(11)(21) **2 378 184**

(12) **BREVET CANADIEN
CANADIAN PATENT**

(13) **C**

(86) Date de dépôt PCT/PCT Filing Date: 2000/08/04
(87) Date publication PCT/PCT Publication Date: 2001/02/15
(45) Date de délivrance/Issue Date: 2009/05/26
(85) Entrée phase nationale/National Entry: 2002/02/01
(86) N° demande PCT/PCT Application No.: US 2000/021299
(87) N° publication PCT/PCT Publication No.: 2001/011380
(30) Priorités/Priorities: 1999/08/05 (US60/147,314);
1999/11/15 (US60/165,564); 2000/05/01 (US60/201,056)

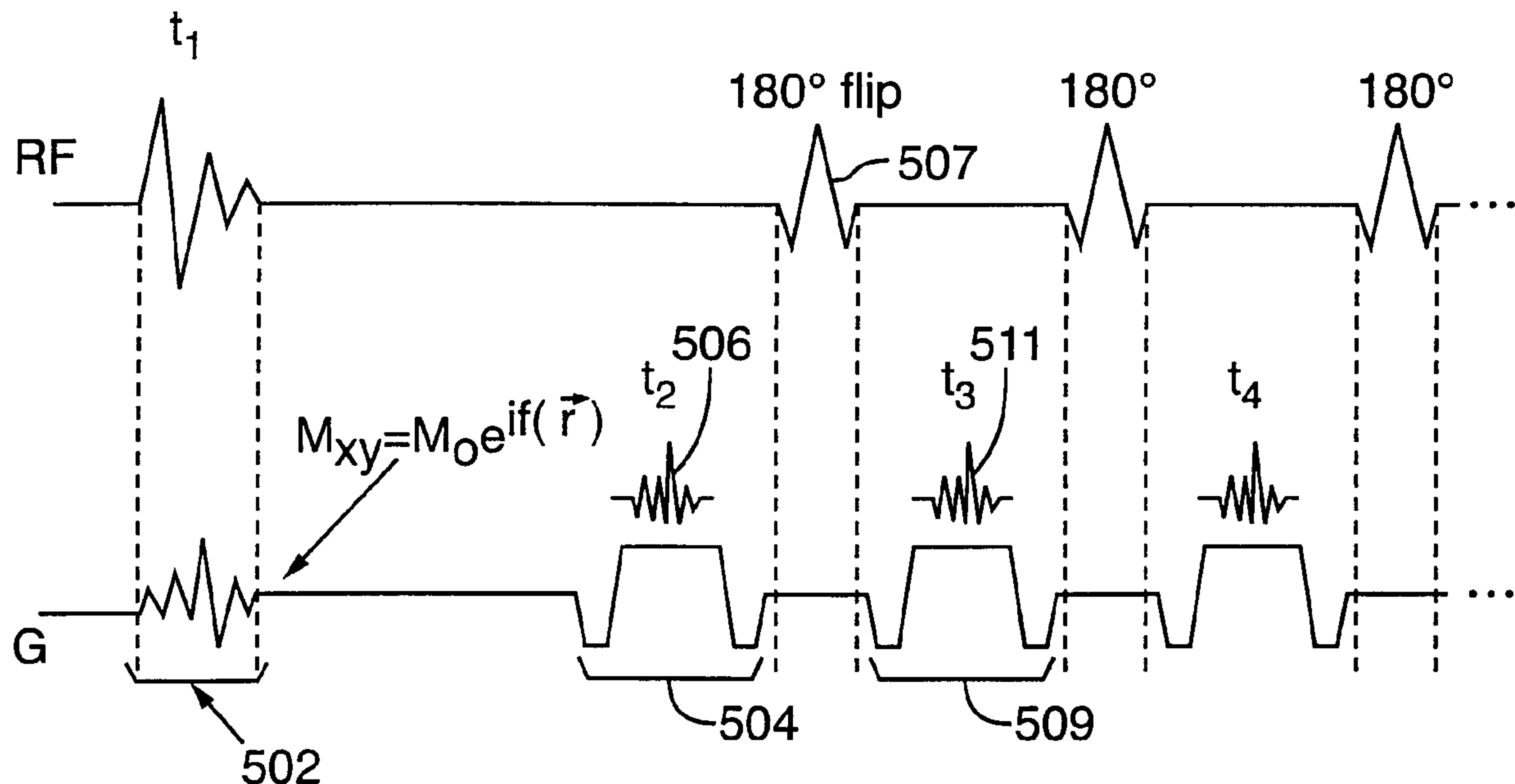
(51) Cl.Int./Int.Cl. *G01R 33/56* (2006.01)

(72) Inventeurs/Inventors:
ALETRAS, ANTHONY H., US;
WEN, HAN, US

(73) Propriétaire/Owner:
THE GOVERNMENT OF THE UNITED STATES OF
AMERICA AS REPRESENTED BY THE
SECRETARY, DEPARTMENT OF HEALTH AND
HUMAN SERVICES, US

(74) Agent: SMART & BIGGAR

(54) Titre : PROCEDES ET APPAREIL PERMETTANT DE MAPPER DES MOUVEMENTS INTERNES ET DES
MOUVEMENTS GLOBAUX D'UN OBJET PAR ETIQUETAGE DE PHASE DANS L'IMAGERIE PAR RESONANCE
MAGNETIQUE
(54) Title: METHODS AND APPARATUS FOR MAPPING INTERNAL AND BULK MOTION OF AN OBJECT WITH
PHASE LABELING IN MAGNETIC RESONANCE IMAGING



(57) Abrégé/Abstract:

Magnetic resonance imaging method and apparatus are provided for mapping the internal or bulk motion of an object by labeling the phase of a specimen magnetization with a selected spatial function and measuring changes in the phase of the magnetization. The special function is selectable to provide magnetization phase modulation corresponding to displacements in a selected direction, such as a radial or azimuthal direction. Methods and apparatus for producing images based on magnetization phase modulation acquire image data based on stimulated echos and stimulated anti-echos. In an embodiment, a series of 180 degree pulses produces alternating stimulated and stimulated anti-echos that are measured and assigned to respective images.

(12) INTERNATIONAL APPLICATION PUBLISHED UNDER THE PATENT COOPERATION TREATY (PCT)

CORRECTED VERSION

(19) World Intellectual Property Organization
International Bureau(43) International Publication Date
15 February 2001 (15.02.2001)

PCT

(10) International Publication Number
WO 01/11380 A3(51) International Patent Classification⁷: G01R 33/483,
33/563[US/US]; The National Institute of Health, Office of
Technology Transfer, Suite 325, 601 Executive Boulevard,
Rockville, MD 20852 (US).

(21) International Application Number: PCT/US00/21299

(72) Inventors; and

(22) International Filing Date: 4 August 2000 (04.08.2000)

(75) Inventors/Applicants (for US only): ALETRAS, An-
thony, H. [US/US]; Apartment 201, 256 Congressional
Lane, Rockville, MD 20852 (US). WEN, Han [US/US];
Apartment 301, 437 West Drive, Gaithersburg, MD 20878
(US).

(25) Filing Language: English

(74) Agent: NOONAN, William, D.; Klarquist, Sparkman,
Campbell, Leigh & Whinston, L.L.P., Suite 1600 - One
World Trade Center, 121 S.W. Salmon Street, Portland, OR
97204 (US).

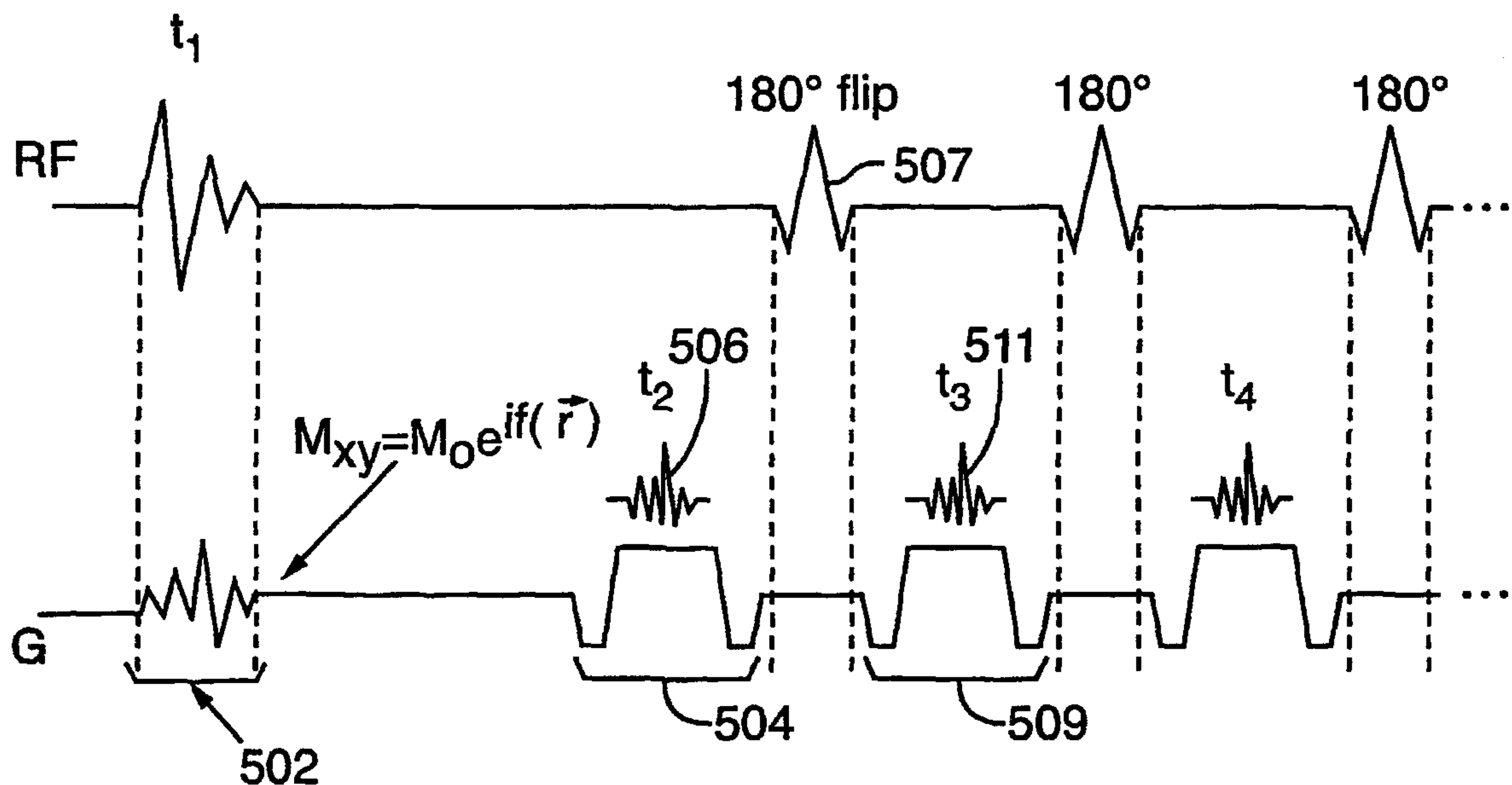
(26) Publication Language: English

(81) Designated States (national): AE, AG, AL, AM, AT, AU,
AZ, BA, BB, BG, BR, BY, BZ, CA, CH, CN, CR, CU, CZ,
DE, DK, DM, DZ, EE, ES, FI, GB, GD, GE, GH, GM, HR,
HU, ID, IL, IN, IS, JP, KE, KG, KP, KR, KZ, LC, LK, LR,
LS, LT, LU, LV, MA, MD, MG, MK, MN, MW, MX, MZ,

(30) Priority Data:

60/147,314 5 August 1999 (05.08.1999) US
60/165,564 15 November 1999 (15.11.1999) US
60/201,056 1 May 2000 (01.05.2000) US(71) Applicant (for all designated States except US): THE
GOVERNMENT OF THE UNITED STATES OF
AMERICA as represented by THE SECRETARY,
DEPARTMENT OF HEALTH & HUMAN SERVICES

[Continued on next page]

(54) Title: METHODS AND APPARATUS FOR MAPPING INTERNAL AND BULK MOTION OF AN OBJECT WITH PHASE
LABELING IN MAGNETIC RESONANCE IMAGING

WO 01/11380 A3

(57) Abstract: Magnetic resonance imaging method and apparatus are provided for mapping the internal or bulk motion of an object by labeling the phase of a specimen magnetization with a selected spatial function and measuring changes in the phase of the magnetization. The special function is selectable to provide magnetization phase modulation corresponding to displacements in a selected direction, such as a radial or azimuthal direction. Methods and apparatus for producing images based on magnetization phase modulation acquire image data based on stimulated echos and stimulated anti-echos. In an embodiment, a series of 180 degree pulses produces alternating stimulated and stimulated anti-echos that are measured and assigned to respective images.

WO 01/11380 A3



NO, NZ, PL, PT, RO, RU, SD, SE, SG, SI, SK, SL, TJ, TM,
TR, TT, TZ, UA, UG, US, UZ, VN, YU, ZA, ZW.

(88) Date of publication of the international search report:
14 June 2001

(84) Designated States (regional): ARIPO patent (GH, GM, KE, LS, MW, MZ, SD, SL, SZ, TZ, UG, ZW), Eurasian patent (AM, AZ, BY, KG, KZ, MD, RU, TJ, TM), European patent (AT, BE, CH, CY, DE, DK, ES, FI, FR, GB, GR, IE, IT, LU, MC, NL, PT, SE), OAPI patent (BF, BJ, CF, CG, CI, CM, GA, GN, GW, ML, MR, NE, SN, TD, TG).

(48) Date of publication of this corrected version:
5 July 2001

(15) Information about Correction:
see PCT Gazette No. 27/2001 of 5 July 2001, Section II

Published:

— With international search report.

For two-letter codes and other abbreviations, refer to the "Guidance Notes on Codes and Abbreviations" appearing at the beginning of each regular issue of the PCT Gazette.

METHODS AND APPARATUS FOR MAPPING INTERNAL AND BULK MOTION OF AN OBJECT WITH PHASE LABELING IN MAGNETIC RESONANCE IMAGING

5

Field of the Invention

The invention pertains to methods and apparatus for magnetic resonance imaging.

Background

Magnetic resonance imaging (“MRI”) is a noninvasive imaging method widely used for medical diagnostics. To date, MRI methods for tracking the motion of an object over relatively long periods of time have been based on spatially 10 modulating magnitude of the specimen magnetization according to a specific grid pattern, and observing the deformation of this grid pattern as motion occurs. In order to quantify the displacement vector of any small volume element (voxel), the 15 positions of the grid lines and their intersection points are precisely defined. This usually requires human assistance, and precision is limited by image resolution or voxel size. The motion of voxels between grid lines cannot be measured directly, and interpolation methods are used to estimate motion.

Other MRI methods measure voxel velocity by subjecting the transverse magnetization to a biphasic gradient pulse before readout, so that stationary spins do 20 not accumulate a net phase change, while spins with nonzero velocity components along the gradient direction accumulate a phase change. By measuring such phase changes, one or more velocity components can be derived. While phase-contrast velocity mapping generally provides high spatial resolution and simple data processing, it is generally unsuitable for motion tracking, as it requires integration of 25 velocity vectors from multiple measurements and mathematically tracking voxel positions. These integrations and voxel position tracking are difficult and prone to error.

63198-1362

2

Summary

Internal and bulk motion of a specimen are mapped by labeling the phase of the specimen magnetization with a selected function of position at an initial time and measuring changes in the phase of the magnetization. Either or both of a

5 longitudinal and a transverse component of specimen magnetization can be phase labeled based on the selected function. A phase labeled component of magnetization is stored by rotating the component to align with a longitudinal axis that is defined by an applied magnetic field. The time varying phase of the specimen magnetization is measured by producing stimulated echos or stimulated anti-echos,

10 or both from the phase labeled magnetization. Measurements of the stimulated echos and the stimulated anti-echos are processed to produce respective images. The phase labeling function can provide a phase modulation based on displacement along any direction. For example, the selected function can be as a function of an azimuthal or other angle, so that rotational displacements produce phase shifts in the

15 specimen magnetization.

'63198-1362

2a

According to one aspect of the present invention, there is provided a magnetic resonance imaging method, comprising: applying a first excitation radio-frequency (RF) pulse along a first excitation axis to produce a first transverse magnetization; applying a first position encoding phase label to the first transverse magnetization; storing a component of the position encoded first transverse magnetization as a first stored longitudinal magnetization by applying a first storing RF pulse along a first storing axis; allowing a first mixing time interval of duration T_M to elapse; after the first mixing time has elapsed, producing a transverse magnetization based on the first stored longitudinal magnetization; decoding the transverse magnetization produced after the first mixing time; generating a first image signal based on the decoded transverse magnetization produced after the first mixing time; applying a second excitation RF pulse along a second excitation axis to produce a second transverse magnetization; applying a second position encoding phase label to the second transverse magnetization; storing a component of the position encoded second transverse magnetization as a second stored longitudinal magnetization by applying a second storing RF pulse along a second storing axis, wherein a difference between an angle from the first excitation axis to the first storing axis and an angle from the second excitation axis to the second storing axis is not an integer multiple of 180 degrees; allowing a second mixing time of duration T_M to elapse; after the second mixing time has elapsed, producing a transverse magnetization based on the second stored longitudinal magnetization; decoding the transverse magnetization produced after the second mixing time; generating a second image signal based on the decoded transverse magnetization produced after the second mixing time; and combining the first image signal and the second image signal.

63198-1362

2b

image signal to reduce a contribution associated with a complex conjugate of a phase-labeled magnetization to obtain an artifact-reduced image of a specimen.

According to another aspect of the present

5 invention, there is provided a magnetic resonance imaging method, comprising: applying a first excitation radio-frequency (RF) pulse along a first excitation axis to produce a first transverse magnetization; applying a first position encoding phase label to the first transverse

10 magnetization; storing a component of the position encoded first transverse magnetization as a first stored longitudinal magnetization by applying a first storing RF pulse along a first storing axis; allowing a first mixing time interval of duration T_M to elapse; after the first

15 mixing time has elapsed, producing a transverse magnetization based on the first stored longitudinal magnetization; decoding the transverse magnetization produced after the first mixing time; generating a first image signal based on the decoded transverse magnetization

20 produced after the first mixing time; applying a second excitation RF pulse along a second excitation axis to produce a second transverse magnetization; applying a second position encoding phase label to the second transverse magnetization; storing a component of the position encoded

25 second transverse magnetization as a second stored longitudinal magnetization by applying a second storing RF pulse along a second storing axis; allowing a second mixing time of duration T_M to elapse; after the second mixing time has elapsed, producing a transverse magnetization based on

30 the second stored longitudinal magnetization; decoding the transverse magnetization produced after the second mixing time; generating a second image signal based on the decoded transverse magnetization produced after the second mixing

63198-1362

2c

time; applying a third excitation RF pulse along a third excitation axis to produce a third transverse magnetization; applying a third position encoding phase label to the third transverse magnetization; storing a component of the 5 position encoded third transverse magnetization as a third stored longitudinal magnetization by applying a third storing RF pulse along a third storing axis, wherein an angle from the first excitation axis to the first storing axis, an angle from the second excitation axis to the second 10 storing axis, and an angle from the third excitation axis to the third storing axis are different; allowing a third mixing time interval of duration T_M to elapse; after the third mixing time has elapsed, producing a transverse magnetization based on the third stored longitudinal 15 magnetization; decoding the transverse magnetization produced after the third mixing time; generating a third image signal based on the decoded transverse magnetization produced after the third mixing time; and combining the first, second, and third image signals to reduce either a 20 contribution associated with a complex conjugate of a phase-labeled magnetization or free induction decay, or both to obtain an artifact-reduced image of a specimen.

According to still another aspect of the present invention, there is provided a magnetic resonance imaging 25 method, comprising: applying an excitation radio-frequency (RF) pulse along an excitation axis to produce a transverse magnetization; applying a position encoding phase label to the transverse magnetization; storing a component of the position encoded transverse magnetization as a stored 30 longitudinal magnetization by applying a storing RF pulse along a storing axis; allowing a mixing time interval of duration T_M to elapse; applying an RF pulse at a time point within the mixing time interval, wherein the time point is

63198-1362

2d

selected to reduce a signal contribution from free induction decay; after the first mixing time has elapsed, producing a transverse magnetization based on the stored longitudinal magnetization; decoding the transverse magnetization
5 produced after the mixing time; generating an image signal of a specimen and producing an associated image of the specimen based on the decoded transverse magnetization produced after the mixing time.

These and other features and advantages are
10 described below with reference to the accompanying drawings.

Brief Description of the Drawings

FIG. 1 is a schematic block diagram of a magnetic resonance (MR) imaging system.

FIGS. 2A-2B illustrate volume element ("voxel")
15 phase labeling based on a function $f(\mathbf{r})$.

FIGS. 3A-3C illustrate phase labeling of a longitudinal and transverse magnetization based on a function $f(\mathbf{r})$.

FIGS. 4A-4C illustrate phase labeling of a longitudinal and transverse magnetization based on a
20 function $f(\mathbf{r})$.

FIG. 5 illustrates RF and gradient (G) pulses applied in a fast spin-echo readout of a phase labeled transverse magnetization.

FIG. 6 illustrates RF and gradient (G) pulses applied in a fast spin-echo readout of a phase labeled longitudinal magnetization.

FIG. 7 is an illustration of k-space regions corresponding to phase factors of a transverse magnetization.

5 FIG. 8 illustrates voxel motion with respect to a non-stationary coordinate system.

FIG. 9 illustrates RF and gradient pulses applied to produce a signal (rx) from a phase labeled specimen, wherein the signal corresponds to a stimulated echo or stimulated anti-echo.

10 FIG. 10 is a block diagram of a dual echo imaging method.

FIG. 11A illustrates RF and gradient pulses applied to an image of a phase labeled specimen in an alternating dual echo imaging method.

FIG. 11B illustrates RF and gradient pulses applied to an image of a phase labeled specimen in a simultaneous dual echo imaging method.

15 FIG. 12 illustrates a magnetization spin wheel.

FIG. 13 is a diagram of a sequence of RF and gradient pulses applied according to an embodiment of a rotating wheel method of acquiring phase labeled data.

20 FIG. 14 illustrates RF and gradient pulses of a dual-echo method configured to reduce free induction decay.

Detailed Description

FIG. 1 is a schematic block diagram of a magnetic resonance imaging (MRI) system 100 that provides images of a specimen. The MRI system 100 includes a controller 102 that is typically programmed by a clinician with a series of commands corresponding to a particular imaging sequence. The command sequences can be entered with a keyboard, a pointing device such as a mouse, or other input device. Command sequences can be stored by the controller 102 for retrieval from a hard disk, floppy disk, or other computer readable media and can be selected from a

menu, so that a clinician can easily select among an imaging protocol from various command sequences.

The MRI system 100 includes an axial magnet controller 104 that controls the spatial homogeneity of an axial magnetic field B_0 with an axial field coil 105. 5 As used herein, the axial magnetic field B_0 is directed along a +z-axis in a xyz coordinate system. A plane parallel to an xy-plane (perpendicular to the z-axis) is referred to as a transverse plane. A gradient controller 106 activates gradient coils 107-109 that produce a magnetic field gradients G_x , G_y , G_z . For convenience, the magnetic field gradients G_x , G_y , G_z are represented generically as G . The magnetic 10 field gradients are typically applied as pulses.

A radio-frequency (RF) transmitter 110 is configured to generate RF pulses that are applied to a transmitter coil 112 to produce a pulsed magnetic field. A receiver coil 114 detects changes in magnetization in the specimen and communicates the detected magnetization changes to an RF receiver 116. The RF 15 receiver 116 processes the detected magnetization changes and provides image data to the controller 102 based on these changes.

A specimen to be imaged is exposed to the axial magnetic field B_0 and a field gradient G selected by the controller 102. An RF pulse is applied to produce a change in magnetization that is detected by the receiver coil 114 and processed by 20 the RF receiver 116. The RF pulse is typically represented as product of a pulse envelope B_1 and a complex exponential $\exp(i\omega_{RF}t)$, wherein t is time, i is the square root of -1, and ω_{RF} is an excitation carrier frequency. The excitation frequency ω_{RF} is generally selected to be approximately equal to a resonance frequency of one or 25 more constituents of the specimen. The resonance frequency ω_0 is proportional to a product of a gyromagnetic ratio γ (a material constant) and a magnitude of the axial field B_0 . By applying a field gradient G with the gradient coils 107-109 so that the specimen is exposed to a non-uniform magnetic field, slices of the specimen can be selected for imaging. Within a selected slice, the resonance frequency ω_{RF} is sufficiently constant so that the RF receiver 116 can reject magnetization changes in 30 non-selected slices by rejecting frequency components corresponding to the non-selected slices. Detecting changes in magnetization slice by slice permits image formation.

With only the axial magnetic field B_0 applied, some magnetic dipoles of sample constituents align with the axial magnetic field B_0 to produce an equilibrium magnetization M_0 that generally has only a $+z$ -directed component. The specimen includes individual magnetic dipoles of dipole moment μ that precess about the direction of B_0 (the z -axis) at the frequency $\omega_0 = \gamma B_0$ that is also referred to as the Larmor frequency. Changes in magnetization are generally described with reference to an xyz coordinate system that rotates about the axial direction at the Larmor frequency. The z -axis of such a rotating coordinate system is the same as the z -axis of a stationary coordinate system while the x -axis and y -axis of the rotating coordinate system rotate in a transverse plane.

Application of a selected RF pulse can rotate a magnetization or one or more components thereof. An RF pulse of duration and magnitude sufficient to produce a 180 degree rotation is referred to as a 180 degree pulse and an RF pulse sufficient to produce a 90 degree rotation is referred to as a 90 degree pulse. In general, an RF pulse sufficient to produce a rotation α is referred to as an α pulse. The axis of rotation of such pulses can be selected based on the direction in which the corresponding pulse magnetic field is applied.

Vector quantities are expressed herein in boldface. A transverse component M_{xy} of a (vector) magnetization \mathbf{M} (i.e., a component of the magnetization \mathbf{M} in the xy-plane) is expressed as $M e^{i\theta}$, wherein an x-component is a real part of $M e^{i\theta}$, a y-component is an imaginary part of $M e^{i\theta}$, and M is a magnitude of the magnetization \mathbf{M} .

Phase Labeling

In some specimens, some volume elements ("voxels") are moving and experience a displacement between an initial time t_1 and a subsequent time t_2 . For example, a portion of a specimen moving parallel to the x -axis acquires an x -directed displacement. The magnetization \mathbf{M} can be encoded (i.e., modulated) based upon such displacements. Such a modulation can be a function of position and can be generally expressed as $f(\mathbf{r}(t_2)) - f(\mathbf{r}(t_1))$, wherein $\mathbf{r}(t_2)$ and $\mathbf{r}(t_1)$ are positions of a voxel at times t_2 and t_1 , respectively, and $f(\mathbf{r})$ is an arbitrary function of position \mathbf{r} .

Modulation of the magnetization based on displacements permits imaging based upon displacement.

The magnetization can be amplitude modulated, frequency modulated, or phase modulated. Phase modulation can be accomplished by modulating the magnetization \mathbf{M} or a component of the magnetization \mathbf{M} with a phase factor $e^{if(r)}$ at a time t_1 , producing a phase modulated magnetization. A phase factor such as $e^{if(r)}$ is referred to herein as a “phase label.” The phase modulated magnetization can be preserved until a time t_2 , when an MR image is acquired based on the phase modulation. A voxel that is displaced to a position $\mathbf{r}(t_2)$ retains a phase factor based on $f(\mathbf{r}(t_1))$ and can be further modulated or demodulated with a phase factor based on $f(\mathbf{r}(t_2))$ to produce an image based on $f(\mathbf{r}(t_2))-f(\mathbf{r}(t_1))$. RF and gradient pulses that provide a selected modulation or phase labeling can be selected to provide phase modulation according to a function $f(\mathbf{r})$.

FIGS. 2A-2B illustrate phase labeling based on a function $f(\mathbf{r}) = kr$, wherein r is a radial coordinate in a cylindrical (r, θ, z) coordinate system and k is a constant. A corresponding phase label is e^{ikr} . With such a phase label, a voxel acquires a phase proportional to a change in radial coordinate between times t_1 and t_2 , i.e., a change in distance between the voxel and an origin of the cylindrical coordinate system. At time t_1 , a phase proportional to kr is applied so that voxel phase as a function of the radial coordinate is $f(r) = kr$ with a corresponding phase label e^{ikr} . At time t_2 , voxels are displaced from voxel positions at time t_1 and the voxel phase label is $e^{i\phi(r)}$. The phase $\phi(r)$ is produced by a combination of the initial phase labeling with e^{ikr} and changes in the phase as a function of position produced by displacements. A radial displacement Δr of a voxel can be obtained from a measurement of the phase $\phi(r)$ as $\Delta r = r - \phi(r)/k$ and a radial coordinate of a voxel at time t_2 is $\phi(r)/k$.

In a Cartesian (x, y, z) coordinate system, the magnetization \mathbf{M} includes a longitudinal component M_z and a transverse component M_{xy} and can be phase labeled in several ways. The longitudinal component M_z can be phase labeled using RF and gradient pulses to apply a modulation $m(\mathbf{r})e^{if(r)}$, wherein $m(\mathbf{r})$ is a real function of position \mathbf{r} , and $f(\mathbf{r})$ is a phase-labeling function. Because the longitudinal magnetization M_z is a scalar, and therefore a real number, the

longitudinal magnetization M_z also contains a complex conjugate term $m(\mathbf{r})e^{-if(\mathbf{r})}$. Alternatively, the transverse component M_{xy} can be labeled with a combination of RF and gradient pulses to include modulations corresponding to $m(\mathbf{r})e^{if(\mathbf{r})}$, $m(\mathbf{r})e^{-if(\mathbf{r})}$, or a combination of both. In addition, both the longitudinal and transverse

5 components can be labeled to include phase-labeled terms such as $e^{if(\mathbf{r})}$, $e^{-if(\mathbf{r})}$, or both.

To produce a transverse magnetization having a selected phase modulation according to a function $f(\mathbf{r})$, the equilibrium magnetization M_0 is typically rotated into the transverse plane with a combination of RF and gradient pulses. Such a

10 pulse combination can be determined based on the following equations for rates of change of M_{xy} and M_z found in, for example, Pauly et al., J. Magn. Resonan. 81:43-56 (1989):

$$\begin{aligned}\dot{M}_{xy} &= -i\gamma\mathbf{G}\cdot\mathbf{r}M_{xy} + i\gamma B_1 M_z, \\ \dot{M}_z &= -\gamma \langle M_{xy} \cdot iB_1 \rangle,\end{aligned}$$

where \mathbf{G} represents an applied magnetic field gradient and B_1 is an amplitude of the

15 RF pulse. By integrating these equations, M_{xy} can be determined as a function of position \mathbf{r} and time t :

$$M_{xy}(\mathbf{r}, t) = i\gamma M_0 \int_0^t B_1(\tau) e^{i\mathbf{r}\cdot\mathbf{k}(\tau)} d\tau + i\gamma^2 \int_0^t d\tau B_1(\tau) e^{i\mathbf{r}\cdot\mathbf{k}(\tau)} \int_0^\tau \langle M_{xy}(\mathbf{r}, s) \cdot iB_1(s) \rangle ds,$$

wherein $\mathbf{k}(t)$ is a k-space trajectory driven by the gradient \mathbf{G} as defined in Pauly et al. If the RF-gradient pulse combination is to produce $M_{xy}(\mathbf{r}, T) = m(\mathbf{r})e^{if(\mathbf{r})}$ at a time

20 T corresponding to the conclusion of the RF-gradient pulse combination, then the RF pulse can be selected so that

$$\int_0^t B_1(\tau) e^{i\mathbf{r}\cdot\mathbf{k}(\tau)} d\tau = -\frac{i}{\gamma M_0} M_{xy}(\mathbf{r}, T) - \frac{\gamma}{M_0} \int_0^T d\tau B_1(\tau) e^{i\mathbf{r}\cdot\mathbf{k}(\tau)} \int_0^\tau \langle M_{xy}(\mathbf{r}, s) \cdot iB_1(s) \rangle ds.$$

If $m(\mathbf{r})$ is small compared to the magnetization M_0 , the small-tip-angle

25 approximation of Pauly et al. can be used and $B_1(t)$ calculated by neglecting the second term in the above equation. For phase labeling in motion/displacement imaging, $m(\mathbf{r})$ is preferably substantially equal to the magnetization M_0 to improve signal-to-noise ratio ("SNR") in phase-label measurements (and to avoid signal contributions from unlabeled magnetization components), and the small-tip-angle

approximation is generally not sufficient. M_{xy} and B_1 can be obtained from a series expansion, wherein a zeroth order term of B_1 is obtained from the small tip angle approximation, and higher order terms are obtained from lower order terms as follows:

$$5 \quad \int_0^T B_{1,n}(t) e^{i\mathbf{r} \cdot \mathbf{k}(t)} dt = -\frac{\gamma}{M_0} \sum_{j+l+m=n-1} \int_0^T d\tau B_{1,j}(\tau) e^{i\mathbf{r} \cdot \mathbf{k}(\tau)} \int_0^\tau \langle M_{xy,l}(\mathbf{r}, s) \cdot iB_{1,m}(s) \rangle ds,$$

$$M_{xy,n}(\mathbf{r}, t) = i\gamma M_0 \int_0^t B_{1,n}(\tau) e^{i\mathbf{r} \cdot \mathbf{k}(\tau)} d\tau + i\gamma^2 \sum_{j+l+m=n-1} \int_0^t d\tau B_{1,j}(\tau) e^{i\mathbf{r} \cdot \mathbf{k}(\tau)} \int_0^\tau \langle M_{xy,l}(\mathbf{r}, s) \cdot iB_{1,m}(s) \rangle ds,$$

wherein j , l m , and n are nonnegative integers, and n is the order of the term obtained, i.e., $B_{1,n}$ and $M_{xy,n}$ are n th order contributions to B_1 and M_{xy} , respectively.

For a specified function $m(\mathbf{r})e^{if(\mathbf{r})}$, the series expansion can be calculated numerically until $M_{xy,n}(\mathbf{r}, t)/M_0 \ll 1$, and the RF-gradient pulse combination is sufficiently approximated to produce a selected transverse magnetization $M_{xy}(\mathbf{r}, T) = m(\mathbf{r})e^{if(\mathbf{r})}$.

10 Although phase labeling is described herein generally with respect to phase labeling with a single function $f(\mathbf{r})$, multiple phase labels can be used to obtain a transverse magnetization $M_{xy}(\mathbf{r}, T) = m_1(\mathbf{r})e^{if1(\mathbf{r})} + m_2(\mathbf{r})e^{if2(\mathbf{r})} + m_3(\mathbf{r})e^{if3(\mathbf{r})} + \dots + m_N(\mathbf{r})e^{ifN(\mathbf{r})}$ that is phase-labeled with respective functions $f_1(\mathbf{r})$, $f_2(\mathbf{r})$, $f_3(\mathbf{r})$, \dots , $f_N(\mathbf{r})$.

15 The longitudinal magnetization M_z can be phase-labeled in several ways. For example, a transverse magnetization $M_{xy}(\mathbf{r}) = m(\mathbf{r})e^{if(\mathbf{r})}$ can be produced with an RF-gradient pulse combination as described above, and a second RF pulse such as a 90 degree pulse or other RF pulse applied along the y -axis. In this example, a 90 degree pulse is used and, for improved SNR, $m(\mathbf{r})$ is configured to be substantially equal to the magnetization M_0 and the resulting longitudinal magnetization is $M_z = [m(\mathbf{r})e^{if(\mathbf{r})} + m(\mathbf{r})e^{-if(\mathbf{r})}]/2$.

20 FIGS. 3A-3C illustrate phase labeling of longitudinal and transverse magnetizations with a specified function $f(\mathbf{r})$. The initial magnetization is the axial magnetization M_0 as shown in FIG. 3A. An RF-gradient pulse combination is applied to rotate the magnetization M_0 into the transverse plane and produce a transverse magnetization $M_{xy} = M_0 e^{if(\mathbf{r})}$ as shown in FIG. 3B, leaving only a small (or no) z -component. A 90° RF pulse is applied along the y -axis, and an x -

component of the magnetization is rotated into the yz -plane. The resulting longitudinal and transverse magnetizations, illustrated in FIG. 3C, are:

$$M_z = [e^{if(r)} + e^{-if(r)}]M_0/2, \text{ and}$$

$$M_{xy} = [e^{if(r)} - e^{-if(r)}]M_0/(2i), \text{ respectively,}$$

5 and are both phase-labeled based on the function $f(r)$.

Another method of producing phase-labeled terms $m(r)e^{if(r)}$ or $m(r)e^{-if(r)}$ in the longitudinal magnetization M_z is to apply an RF-gradient pulse combination based on Pauly et al.'s small-tip-angle approximation.

Generally the RF-gradient pulse combinations produce phase modulations of 10 the form $m(r)e^{if(r)}$ and $m(r)e^{-if(r)}$ on both the transverse and longitudinal magnetizations. As shown in FIG. 4A, an RF-gradient pulse combination is applied to rotate the magnetization M_0 into the xy -plane and produce a transverse magnetization $M_{xy} = M_0e^{if(r)}$ and no axial magnetization. As shown in FIG. 4B, a 90° RF pulse is applied about an axis AX at an angle ϕ from the x-axis. A 15 component of M_{xy} perpendicular to the axis AX is rotated into a vertical plane at an angle ϕ relative to the x-axis and a component of M_{xy} parallel to the axis AX remains in the xy -plane along the axis AX. The longitudinal and transverse magnetizations, illustrated in FIG. 4C, are $M_z = M_0\{e^{i[f(r)-\phi]} - e^{-[if(r)-\phi]}\}/(2i)$, and 20 $M_{xy} = M_0\{e^{i[f(r)-\phi]} + e^{-[if(r)-\phi]}\}e^{i\phi}/2$. The presence of the phase angle ϕ in the terms $e^{i[f(r)-\phi]}$ and $e^{-i[f(r)-\phi]}$ provides a method for separating these terms, i.e., by subtracting MRI signals that are acquired with $\phi = \phi_1$ and $\phi = \phi_2$.

Examples of Phase Labeling

In a first example, the selected function of displacement is equal to a 25 Cartesian component of voxel displacement. For example, if the x-component is selected, the phase difference is proportional to $f(r(t_2))-f(r(t_1)) = k(x(t_2)-x(t_1))$, wherein k is a nonzero constant. The corresponding phase label is the function e^{ikx} and a transverse magnetization modulated with this phase label is produced by applying a 90° RF pulse (either slice-selective or volumetric) along the x-axis, followed by a gradient pulse along the x-axis and having an area corresponding to k . 30 The resulting transverse magnetization is $M_{xy} = M_0e^{ikx}$. Another 90° RF pulse is

applied along the axis AX at an angle ϕ from the x-axis so that both M_z and M_{xy} include phase-labeled terms:

$$M_z = M_0[e^{i(kx-\phi)} - e^{-i(kx-\phi)}]/(2i), \text{ and}$$

$$M_{xy} = M_0[e^{i(kx-\phi)} + e^{-i(kx-\phi)}]/2.$$

5 Such phase labeling is readily configurable to phase modulate corresponding to a projection of the displacement vector along an arbitrary direction.

The function $f(r)$ can also be specified in cylindrical, spherical, or other coordinates. As a second example, voxels can be phase labeled based on a radial displacement r in cylindrical coordinates with a function $f(r) = kr$, wherein k is a 10 constant. The series expansion described above can be used to determine an appropriate RF-gradient pulse combination to produce $M_{xy} = m(r)e^{ikr}$. The resulting transverse magnetization M_{xy} can be configured so that $m(r) = 0$ for $r = 0$ so that the Fourier transform of M_{xy} is well defined and the series expansion for the RF-gradient pulse combination converges. As with the function kx in Cartesian 15 coordinates, a 90° RF pulse is applied about an axis AX at an angle ϕ from the x axis after producing the transverse magnetization $M_{xy} = m(r)e^{ikr}$ so that both M_z and M_{xy} are phase-labeled:

$$M_z = M_0[e^{i(kr-\phi)} - e^{-i(kr-\phi)}]/(2i), \text{ and}$$

$$M_{xy} = M_0[e^{i(kr-\phi)} + e^{-i(kr-\phi)}]/2.$$

20 Such phase-labeling is especially useful for mapping changes in the diameter or size of an object relative to a central axis, such as measuring a radial contraction or dilation of a left ventricle of a heart.

The function $f(r)$ can also be selected to be a function of the θ -coordinate (azimuthal angle) in a cylindrical coordinate system to label angular displacements, 25 i.e., $\theta(t_2) - \theta(t_1)$. In a third example, a representative phase labeling function is $f(r) = n\theta$, wherein n is a nonzero integer. Phase-labeling is performed as above except the RF-gradient pulse combination is determined using the function $m(r)e^{in\theta}$. This function is useful for mapping rotations, about a central axis. For example, such a function can be used in MRI of a cross-section of a left ventricle of the heart to 30 produce images based on rotations of the left ventricle and angular changes in segments of the left ventricle.

Mapping the Time-Evolution of a Phase Label

The evolution of voxel phase after an initial phase labeling at time t_1 can be determined by detecting voxel phase at a subsequent time t_2 . If the phase label is applied to the transverse magnetization as $M_{xy} = m(r)e^{if(r)}$, and the time period 5 between t_1 and t_2 is short enough so that the transverse magnetization M_{xy} does not entirely decay due to spin relaxation processes such as T_2^* relaxation, then at time t_2 an image based on the transverse magnetization M_{xy} can be directly acquired with standard gradient-recalled-echo (GRE) or spin-echo readout (SPE) methods, or variants such as spoiled gradient-recalled echo, fast-spin-echo, echo-planar, echo-10 train, k-space spiral scan, true free imaging in steady precession (FISP), and others. The spatial distribution of the phase of the transverse magnetization M_{xy} corresponds to the phase label.

FIG. 5 illustrates acquisition of image data based on a phase-labeled transverse magnetization M_{xy} using a fast spin-echo readout in which the transverse magnetization M_{xy} is acquired at a series of times t_n . At a time t_1 , an RF-gradient pulse combination 502 produces a transverse magnetization $M_{xy} = M_0e^{if(r)}$ that is sampled at time t_2 by applying a fully balanced readout gradient pulse 504 to produce a first echo 506. The balanced readout gradient pulse 504 is compensated to produce no net phase shift. A 180° RF pulse 507 is then applied, followed by 15 balanced readout gradient pulse 509, producing a second echo 511. The 180° RF pulse and the balanced readout gradient pulse are repeated, producing additional echoes. 20

Various exemplary acquisition methods are described herein that are suitable for measuring phase labeled transverse or longitudinal magnetizations (or both) that 25 contain phase labels such as $e^{-if(r)}$ and $e^{if(r)}$. A phase-labeled longitudinal magnetization $M_z = [m(r)e^{i[f(r)-\phi]} - m(r)e^{-i[f(r)-\phi]}]/(2i)$ at time t_1 can be detected by applying an RF-gradient pulse combination at a time t_2 to produce a spatial phase distribution $A(r) = a(r)e^{-if(r)}$, wherein $a(r)$ is a real function of position r . The spatial phase distribution $A(r)$ provided by the RF-gradient pulse combination is selected to 30 correspond to the phase-label applied at time t_1 . Such RF-gradient pulse combinations can be selected using the series expansion described above. The resulting transverse magnetization is:

$$M_{xy}(r) = a(r) \{ m(r') e^{i[f(r(t1))-f(r(t2))-\phi]} - m(r') e^{-i[f(r(t1))+f(r(t2))-\phi]} \} / (2i).$$

For some phase-labeling functions $f(r)$, the two terms in the above equation have little overlap in Fourier transform space (“k-space”), and data corresponding to the first term can be isolated by acquiring $M_{xy}(r)$ over a k-space region encompassing 5 primarily the first term. The acquisition can be of any of the standard gradient-recalled echo or spin-echo schemes, or variants thereof. The phase of the first term in M_{xy} includes $f(r')-f(r)$. The RF-gradient pulse combination that produces $A(r)$ is referred to as a “decoding pulse.”

FIG. 6 illustrates data acquisition using a decoding pulse and a fast spin-echo 10 readout. At time t_1 , an RF-gradient pulse combination 602 produces a phase-labeled transverse magnetization $M_z = [e^{if(r)} - e^{-if(r)}]M_0/(2i)$. A spoiler gradient pulse 604 is applied to dephase the coherent transverse magnetization. At time t_2 , an RF-gradient decoding pulse 606 produces a tip angle of the spatial distribution $a_0 e^{-if(r)}$. The resulting transverse magnetization is:

$$15 \quad M_{xy}(r) = a_0 M_0 \{ e^{i[f(r(t1))-f(r(t2))]} - e^{-i[f(r(t1))+f(r(t2))]} \} / (2i).$$

This magnetization is then sampled with a fully balanced readout gradient pulse 608 to produce an echo 610. A 180° RF pulse 612 is applied, changing the sign of the phase factors in the transverse magnetization so that $M_{xy}(r)$ is:

$$M_{xy}(r) = a_0 M_0 \{ e^{-i[f(r(t1))-f(r(t2))]} - e^{i[f(r(t1))+f(r(t2))]} \} / (2i)$$

20 and the balanced readout gradient pulse / 180° RF pulse sequence is repeated. If the two terms in M_{xy} have little k-space overlap, only the area of k-space encompassing the first term is sampled. To compensate for sign changes of the phase factors produced by 180° RF pulses, a complex conjugate of data from every other readout period is obtained and assigned to an opposite location in k-space.

25 As shown in FIG. 6, between times t_1 and t_2 , the spoiler pulse 604 is applied to destroy the coherence in M_{xy} left by the RF-gradient pulse combinations at time t_1 . Alternatively, if the time period between t_1 and t_2 is sufficiently long so that the coherence in M_{xy} decays to negligible levels, then such a spoiler gradient pulse is unnecessary.

30 This acquisition method can be further illustrated with the example of the phase-labeling function $f(r) = kr$, in cylindrical coordinates. After the decoding RF-gradient pulse combination that produces $A(r)$ is applied, the terms in M_{xy} have

phase factors $e^{i[k(r(t_1)-r(t_2))-\phi]}$ and $e^{i[k(r(t_1)+r(t_2))-\phi]}$. If the specimen does not experience large or abrupt deformations or displacements, changes, but a continuous or gradual deformation, the second term oscillates radially at a high spatial frequency of approximately $2k$, while the first term has a nearly zero frequency oscillation.

5 Referring to FIG. 7, the Fourier transform of the first term is concentrated at $k = 0$ in a region 702, while the Fourier transform of the second term is at a distance greater than or equal to $2k$ from the origin in a region 704. If k is sufficiently large, these 10 two regions have little or no overlap in k -space. In MRI, sampling $M_{xy}(\mathbf{r})$ with a series of readout gradients is equivalent to sampling the Fourier transform of $M_{xy}(\mathbf{r})$ in k -space. Therefore, $M_{xy}(\mathbf{r})$ can be sampled in k -space near the origin ($k = 0$) to include contributions from the term having phase factor $e^{i[k(r(t_1)-r(t_2))-\phi]}$. After an inverse Fourier transform, the corresponding image includes contributions based on $k(r(t_2)-r(t_1))$.

15 Generally, by using an RF-gradient pulse combination $A(\mathbf{r})$ to tip the magnetization M_z onto the xy plane and selecting a phase of $A(\mathbf{r})$ to have a sign opposite that of one of the phase-labeled terms in M_z , the phase of a magnetization tipped onto the transverse plane contains $f(\mathbf{r}(t_2))-f(\mathbf{r}(t_1))$. By acquiring data corresponding to this term, images based on $f(\mathbf{r}(t_2))-f(\mathbf{r}(t_1))$ can be produced.

20 In the above example, $k(r(t_2)-r(t_1))$ is proportional to the radial distance change between the voxel and the central axis. In certain applications, such as mapping the radial contraction and dilation of the left ventricle relative to a long axis of the left ventricle, the position of the long axis generally changes with time as is illustrated in FIG. 8. In this case, a prior MRI scan can be used to locate ventricle positions 801, 803 at times t_1 and t_2 , respectively. Then, the RF-gradient pulse 25 combination that applies the selected phase label can be calculated with respect to the axis position at the initial time t_1 , while the decoding RF-gradient pulse combination can be calculated with respect to the axis position at the time of decoding. Then, $\mathbf{r}(t_1)$ and $\mathbf{r}(t_2)$ are radial distances to the long axis of the left ventricle at times t_1 and t_2 points from the same voxel of the myocardium, and 30 $k(r(t_2)-r(t_1))$ represents radial dilation/contraction regardless of the translational movement of the heart.

Data can also be acquired based on a phase-labeled longitudinal magnetization, such as $M_z = \{m(\mathbf{r})e^{i[f(\mathbf{r})-\phi]} - m(\mathbf{r})e^{-i[f(\mathbf{r})-\phi]}\}/(2i)$. Between times t_1 and t_2 , a series of spoiler gradient pulses (or a single spoiler pulse) is applied to reduce or eliminate coherence in the transverse magnetization left by the encoding RF gradient pulse combination at t_1 . Alternatively, if the time period between t_1 and t_2 is 5 sufficiently long so that the coherence in M_{xy} decays to negligible levels, then the spoiler gradient pulses are not needed. At time t_2 , a standard MRI sequence (e.g., GRE or SPE) is used to acquire an image based on the transverse magnetization of M_{xy} . Then another phase labeling is performed with a different phase constant ϕ' by 10 changing the direction of the RF pulses and another image based on the transverse magnetization M_{xy} is acquired the same way. Denoting the original voxel position as $\mathbf{r}(t_1) = \mathbf{r}'$, then

$$M_{xy}(\mathbf{r}) = \{m(\mathbf{r}')e^{i[f(\mathbf{r}')-\phi]} - m(\mathbf{r}')e^{-i[f(\mathbf{r}')-\phi]}\}/(2i) \text{ and}$$

$$M_{xy,2}(\mathbf{r}) = \{m(\mathbf{r}')e^{i[f(\mathbf{r}')-\phi']} - m(\mathbf{r}')e^{-i[f(\mathbf{r}')-\phi']}\}/(2i).$$

15 Based on these equations, $m(\mathbf{r}')e^{if(\mathbf{r}')}$ can be determined as

$$m(\mathbf{r}')e^{if(\mathbf{r}')} = [M_{xy,2}(\mathbf{r})e^{i\phi} - M_{xy}(\mathbf{r})e^{i\phi'}]/\sin(\phi - \phi'),$$

and therefore the phase-label function $f(\mathbf{r}')$ can be obtained as the phase of $m(\mathbf{r}')e^{if(\mathbf{r}')}$ and the function of displacement $f(\mathbf{r}')-f(\mathbf{r})$ can also be obtained. This method is particularly suited to phase labels such as $e^{in\theta}$ for which modulations corresponding 20 to the phase labels $e^{-if(\mathbf{r})}$ and $e^{if(\mathbf{r})}$ are not well separated in k-space.

Phase-labeled Longitudinal Magnetization Acquisition Method

The longitudinal magnetization can be phase labeled to be

$M_z = \{m(\mathbf{r})e^{i[f(\mathbf{r})-\phi]} - m(\mathbf{r})e^{-i[f(\mathbf{r})-\phi]}\}/(2i)$ at time t_1 . Between times t_1 and t_2 , a series of 25 spoiler gradient pulses can be applied to destroy the coherence in M_{xy} left by the encoding pulses at t_1 . Alternatively, if the time period between t_1 and t_2 is sufficiently long so that the coherence in M_{xy} decays to negligible levels, then the spoiler gradient pulses are not needed. If the two terms in M_z have little overlap in k-space, as for example in $f(\mathbf{r}) = k_x x + k_y y$ where k_x and k_y are large, then at time t_2 , 30 a standard GRE or SPE method or their variants can be used to acquire a region in k-space that encompasses both terms. The two terms are then reconstructed from their respective regions in k-space. The phase factor $e^{if(\mathbf{r}')}$ can then be obtained from

either one of two terms, or from the phase difference between the two terms. Once $f(r')$ is known, the desired function of displacement $f(r') - f(r)$ is obtained. The two phase-labeled terms $m(r)e^{if(r)}$ and $m(r)e^{-if(r)}$ are conventionally called a stimulated echo (STE) and a stimulated anti-echo (STAE).

5 If the two terms in M_z are sufficiently separated in k-space, a gradient-recalled echo method or a modified spin-echo readout method, or their variants, can also be used to collect only the region in k-space that corresponds to one of the two terms. The phase of this single term then contains $f(r')$, and the desired function $f(r') - f(r)$ can be obtained.

10

Example Mapping of Phase Label Time Evolution

Phase labels can be mapped as a function of time to track motion tracking over a period of time. At each time point after the initial phase labeling, a fraction of the longitudinal magnetization is tipped onto the transverse plane, and the 15 resulting transverse magnetization is detected with any of the methods described herein. After data acquisition, the remaining transverse magnetization can be destroyed with gradient spoiler pulses, and this procedure repeated again. The process can be repeated until the phase-labeled longitudinal magnetization is expended. To ensure that only a fraction of the phase-labeled M_z is used each time, 20 the tip angle of the decoding RF-gradient pulses preferably small compared to 90° , e.g., 30° .

For such motion tracking, the phase labeling is performed with a 90° RF pulse, a gradient pulse along the x direction, and a second 90° pulse. This creates the longitudinal magnetization $M_z = (e^{ikx} - e^{-ikx})M_0/(2i)$. A spoiler gradient pulse is 25 then applied to destroy the coherent transverse magnetization. At time t_2 , a small flip angle α pulse tips a portion of the longitudinal magnetization into the transverse plane, where it is sampled repeatedly with a fast spin-echo readout scheme. The readout gradient waveforms of the fast spin-echo scheme are fully balanced to avoid any phase addition to the phase-label function. Then a spoiler gradient can be 30 applied to crush any residual transverse magnetization, before this process is repeated again for the next time point. This process is repeated for a series of time points, until the phase-labeled terms in the longitudinal magnetization are exhausted.

Example Mapping of Displacement with Phase Labeling

A specific example of phase labeling is described with reference to cardiac functional imaging based on displacement encoding with stimulated echoes ("DENSE"). A phase labeling function $f(\mathbf{r})$ is selected that is a dot product of \mathbf{r} and a vector \mathbf{k} such that the phase-labeling function is $f(\mathbf{r}) = k_x x + k_y y + k_z z$, wherein k_x , k_y and k_z are constants. Phase-labeled terms corresponding to $m(\mathbf{r})e^{if(\mathbf{r})}$ and $m(\mathbf{r})e^{-if(\mathbf{r})}$ are referred to as a stimulated echo ("STE") and a stimulated anti-echo ("STAE"). A stimulated echo is generally compensated for phase shifts caused by magnetic field inhomogeneity, chemical shifts, and off-resonance effects and is nearly equivalent to a spin-echo except for the signal loss due to T_1 during a mixing time ("TM"). In order to acquire an STE, two gradient field pulses of equal gradient moment and of the same polarity are used during the echo time ("TE"). In contrast, a stimulated anti-echo (STAE) can be produced with gradient pulses of opposite polarities. An STAE resembles a gradient-recalled echo instead of a spin-echo and carries phase accumulated due to magnetic field inhomogeneities, chemical shifts, and off-resonance effects.

Referring to FIG. 9, a magnetization vector \mathbf{M} is first tipped onto the transverse plane with a first 90° pulse 901. The magnetization \mathbf{M} is described in a complex representation as:

$$20 \quad M[\cos(\phi) + i \sin(\phi)] = M e^{i\phi} \quad [1]$$

wherein M is an amplitude and ϕ a phase of the magnetization \mathbf{M} as it precesses onto the xy -plane. In the laboratory frame of reference, the phase ϕ in is given by:

$$\phi = \gamma B_0 t + \omega_{OFF} t + \gamma \Delta B_0 t + \gamma m r \quad [2]$$

wherein ω_{OFF} is the off-resonance offset, ΔB_0 is an inhomogeneity in B_0 , and m is a gradient field moment or area. In this example, the gradient field moment is defined as $m = G t_G$ wherein G is the amplitude of an equivalent rectangular gradient pulse and t_G is a pulse duration of the equivalent pulse. In the rotating frame of reference, $\gamma B_0 t$ is zero. Off-resonance, main field inhomogeneity and chemical shift phase accumulations have similar time dependence and a total S of these phase shifts is:

$$30 \quad S = \omega_{OFF} t + \gamma \Delta B_0 t. \quad [3]$$

Therefore, in the rotating frame of reference, the total phase is:

$$\phi = S + \gamma m r. \quad [4]$$

During STEAM imaging, all 90° pulses are applied along the same axis (for example along +y), during the first half 902 of an echo time (TE/2) and a phase

$$\varphi_1 = S_1 + \gamma m_1 r_1 \quad [5]$$

5 accumulates. A second 90° pulse 903 rotates a component of magnetization perpendicular to B_1 , (the x-component) back to the z-axis. Gradient spoiler pulses (not shown in FIG. 9) applied during the mixing time TM scramble components of magnetization remaining in the transverse plane. Because the gradient pulse 910 during the first half of the echo time TE distributes the magnetization components 10 evenly between the real (x) and the imaginary (y) axes, one half of the magnetization is lost. The magnetization relaxes with time constant T_1 . In addition, the phase of the scrambled portion is lost, and a direction of precession of the magnetization can no longer be uniquely determined. If an imaginary part of the magnetization is 15 scrambled and lost (i.e., a y-component), only $M \cos(\varphi_1) = M \cos(S_1 + \gamma m_1 r)$ is restored onto the transverse plane following a third 90° RF pulse 905. This magnetization can be written as

$$\begin{aligned} M \cos(\varphi_1) &= \frac{M}{2} e^{i\varphi_1} + \frac{M}{2} e^{-i\varphi_1} = \\ &= \frac{M}{2} [\cos(\varphi_1) + i \sin(\varphi_1)] + \frac{M}{2} [\cos(-\varphi_1) + i \sin(-\varphi_1)] \end{aligned} \quad [6]$$

20 The nonscrambled real portion of the signal along the x-axis can be considered as the sum of two vectors precessing at the same rate, but in opposite directions. Each of them has half the amplitude of the original magnetization vector.

The magnetization described by Equation 6 is missing phase imparted to the 25 spins by the 90° pulses. For this description of STEAM, the second and third 90° pulses in the RF pulsing scheme (90°_Y - 90°_Y - 90°_Y) behave as a 180° pulse because the magnetization rotates 180° as a result of their application. A 180° pulse changes the sign of the phase since the signal is multiplied by e^{-i} . After the application of a 180° pulse, the resulting magnetization is the complex conjugate of the original magnetization, i.e., its phase changes sign. For an RF pulse scheme 90°_Y - 90°_Y - 90°_Y, there is no sign change. After the 90° pulse 905, the phase of the magnetization is:

$$\varphi_1 = -S_1 - \gamma m_1 r_1 \quad [6a]$$

During the second half 904 of the echo time TE an additional phase φ_2 accumulates, wherein

$$\varphi_2 = +S_2 + \gamma m_2 r_2. \quad [7]$$

5 At a center of an acquisition window 906, the transverse magnetization is:

$$\begin{aligned} M \cos(\varphi_1) e^{i\varphi_2} = \\ \left\{ \frac{M}{2} e^{i\varphi_1} + \frac{M}{2} e^{-i\varphi_1} \right\} e^{i\varphi_2} = \frac{M}{2} e^{i(\varphi_1 + \varphi_2)} + \frac{M}{2} e^{i(-\varphi_1 + \varphi_2)} = \\ \frac{M}{2} [\cos(\varphi_1 + \varphi_2) + i \sin(\varphi_1 + \varphi_2)] + \frac{M}{2} [\cos(-\varphi_1 + \varphi_2) + i \sin(-\varphi_1 + \varphi_2)] \end{aligned} \quad [8]$$

Gradient pulses 910, 912 are characterized by respective amplitudes m_1, m_2 and a duration t_G . Typically, $m_1=m_2$ and $S_1=S_2$ since the echo interval TE is divided into two equal parts. Therefore, for stationary spins, $\phi_1+\phi_2=0$ and (-

10 $\phi_1+\phi_2)=2S_1+2\gamma m_1 r_1$. The detected signal is obtained from the magnetization

$$\frac{M}{2} + \frac{M}{2} [\cos(2S_1 + 2\gamma m_1 r_1) + i \sin(2S_1 + 2\gamma m_1 r_1)] \quad [9]$$

The signal consists of two parts. The first part corresponds to an STE since no residual phase exists as a result of the time-dependent terms described by S and resembles a spin-echo. The second part is modulated by twice the phase imparted
15 by the gradient moment m_1 . In imaging experiments, m_1 is typically large enough to shift this component outside the region of k-space sampled to create an image.

Otherwise, banding artifacts can appear. For non-stationary spins ($r_2 = r_1 + \delta$), then $\phi_1+\phi_2 = \gamma m_1 \delta$ and $(-\phi_1+\phi_2) = 2S_1 + 2\gamma m_1 r_1 + \gamma m_1 \delta$. Therefore, the detected signal consists of a DENSE signal and an m_1 modulated component that is filtered out.

20 The DENSE signal is:

$$\frac{M}{2} [\cos(\gamma m_1 \delta) + i \sin(\gamma m_1 \delta)] = \frac{M}{2} e^{i\gamma m_1 \delta}. \quad [10]$$

On the other hand, if two gradient pulses 910, 914 of opposite signs are applied, the signal changes. With stationary spins $m_1 = -m_2$, and $S_1 = S_2$, then $\phi_1+\phi_2 = -2\gamma m_1 r_1$ and $(-\phi_1+\phi_2) = 2S_1$. Therefore, the signal detected is an STAE and corresponds to:

$$25 \quad \frac{M}{2} [\cos(-2\gamma m_1 r_1) + i \sin(-2\gamma m_1 r_1)] + \frac{M}{2} [\cos(2S_1) + i \sin(2S_1)]. \quad [11]$$

A filter prior to a Fourier transform removes signal contributions modulated by m_1 . The remaining signal portion is modulated by the time-varying terms (S) such as field inhomogeneity, etc., and is similar to a gradient-echo. If the spins are not stationary ($r_2=r_1+\delta$), then $\phi_1+\phi_2=-2\gamma m_1 r_1 - \gamma m_1 \delta$, and $(-\phi_1+\phi_2)=2S_1 - \gamma m_1 \delta$. Thus, 5 the signal portion that is passed by the Fourier transform filter is an STAE and corresponds to:

$$\frac{M}{2} [\cos(2S_1 - \gamma m_1 \delta) + i \sin(2S_1 - \gamma m_1 \delta)] = \frac{M}{2} e^{i(2S_1 - \gamma m_1 \delta)}. \quad [12]$$

The STAE in a DENSE experiment reflects displacement δ that occurs between the two gradient pulses in the TE period but it is contaminated by the time varying terms 10 (S). This is the reason for selecting the STE not the STAE as the STEAM signal when performing such measurements. The STE is not totally free of influence by the time-varying terms. Because the spins move, the contributions of these terms during the first half 902 of TE are not equal to those during the second half 904 of TE. In a more accurate description, $S_1 \neq S_2$.

15 To describe phase label measurements, phases of two components of the signal magnetization can be written as ordered pairs. For example, the signal stored along the longitudinal axis after the second 90° pulse, as described by Equations 5 and 6, can be expressed as

$$\{\varphi_1, -\varphi_1\} = \{S_1 + \gamma m_1 r_1, -S_1 - \gamma m_1 r_1\} \quad [12a]$$

20 Referring to FIG. 9, the signal magnetization after the gradient pulse 912 is described by Equation 9 and can be written as $\{0, 2S_1 + 2\gamma m_1 r_1\}$. In the case of moving spins, where $S_1 \neq S_2$ and $r_2 = r_1 + \delta$, the STE can be written as:

$$\{-S_1 + S_2 + \gamma m_1 \delta_1, S_1 + S_2 + \gamma m_1 \delta + 2\gamma m_1 r_1\} \quad [13]$$

As discussed previously, only the first term is detectable while the second is 25 modulated by $2\gamma m_1 r_1$ and is filtered out before the Fourier transform. The detected portion corresponds to an STE. A more complete description of a STEAM signal in the presence of motion and gradient pulses of opposite polarity is:

$$\{-S_1 + S_2 - 2\gamma m_1 r_1 - \gamma m_1 \delta, S_1 + S_2 - \gamma m_1 \delta\} \quad [14]$$

The first term is undetectable since it is modulated by $\gamma m_1 r_1$, while the second term 30 corresponds to an STAE.

The fast spin echo (FSE) measurement shown in FIG. 9 can cause severe image artifacts when used to rapidly sample a STEAM signal because the signal phase changes sign with every 180° pulse. These image artifacts can be avoided with a dual echo method.

5 FIG. 10 is a block diagram of a dual echo method of displacement imaging. An axial magnetic field B_0 is established in a step 1002 to produce a +z-directed magnetization M_0 . In a step 1004, a 90 degree pulse is applied with the y-axis as the axis of rotation, rotating the magnetization M_0 to the x-axis. A magnetic field gradient $+G_x$ is applied in a step 1006 for a duration t_G , shifting the Larmor frequency by $\gamma G_x x_1$. This frequency shift produces a phase shift proportional to $\gamma G_x t_G x_1$ where $m_1 = G_x t_G$; and rotates the magnetization M_0 from the x-axis by an angle $\gamma m_1 x_1$. In addition, during t_G an additional time-dependent phase shift S_1 is produced by an off-resonance frequency offset ω_{OFF} , and the inhomogeneity ΔB_0 in the axial field B_0 and the phase shift $S_1 = \omega_{OFF} t_G/2 + \gamma \Delta B_0 t_G/2$. Upon 10 completion of the step 1006, the magnetization is in the transverse plane and is represented as $M_0 \exp[i(\gamma m_1 x_1 + S_1)]$. In a step 1008, a second 90 degree pulse is applied along the y-axis to rotate an x-component (i.e., the real part) of the magnetization $M_0 \exp[i(\gamma m_1 x_1 + S_1)]$ to the z-axis and a y-component of the magnetization is unchanged. Typically, the y-component decays rapidly with a time 15 constant referred to as T_2^* . As a result of the second 90 degree pulse and the decay of the y-component of magnetization, the remaining magnetization is z-directed with a magnitude that is proportional to $M_0 \cos(\gamma m_1 x_1 + S_1)$. For convenience, $\cos(\phi_1 + S_1)$ can be expressed as a sum of complex exponentials so that the magnetization is $M_0 [\exp(i\phi_1 + S_1) + \exp(-i\phi_1 - S_1)]/2$.

20

25 In a step 1010, a mixing time T_M is provided in which no additional magnetic fields are applied. During the mixing time T_M , dipole moments associated with moving voxels of the sample experience displacements. After the mixing time T_M , a third 90 pulse is applied in a step 1012, rotating the magnetization vector back into the transverse plane. A first compensation interval of duration $t_2/2$ is provided in a 30 step 1014. During the first compensation interval, no additional magnetic fields are applied but a phase shift S_2 is produced by the off-resonance frequency offset ω_{OFF}

and the magnetic field inhomogeneity ΔB_0 . The phase shift $S_2 = \omega_{OFF} t_2/2 + \gamma \Delta B_0 t_2/2$.

5 A 180 degree pulse is applied in a step 1016, rotating the magnetization in the xy -plane such that the x -component experiences a 180° phase shift. A magnetic field gradient of magnitude $-G$ is then applied for a duration t_G in a step 1018 and produces a phase shift proportional to $-Gt_{GX} = -\gamma m_2 x_2$. A second compensation interval $t_2/2$ is provided in a step 1020. An echo is detected in a step 1022 and data are processed in a step 1024.

10 In a step 1026, a compensation interval $t_2/2$ is provided and in a step 1028 a gradient $+G$ is applied for a duration t_G . Steps 1026, 1028, 1018, 1020 are repeated to provide additional echos in order to form an image. The number of echos is limited by T_2 relaxation.

15 Table 1 illustrates the phase shifts produced by the method of FIG. 10, wherein $\cos\phi$ is represented as a sum of $\exp(-i\phi)$ and $\exp(i\phi)$.

Table 1. Phase shifts associated with the method of FIG. 10 for $m_1 = m_2$.

Step No.	Phase Source	-phase term	+phase term
1012	90 degree pulse	$-S_1 - \gamma m_1 x_1$	$S_1 + \gamma m_1 x_1$
1014	$t_2/2$	$-S_1 + S_2 - \gamma m_1 x_1$	$S_1 + S_2 + \gamma m x_1$
1016	180 degree pulse	$S_1 - S_2 + \gamma m_1 x_1$	$-S_1 - S_2 - \gamma m_1 x_1$
1018	-gradient	$S_1 - S_2 - \gamma m \delta$	$-S_1 - S_2 - \gamma m \delta - 2\gamma m x$
1020	$t_2/2$	$S_1 - \gamma m \delta$	$-S_1 + \gamma m \delta - 2\gamma m x_2$
1022		Echo	
1026	$t_2/2$	$S_1 + S_2 - \gamma m \delta$	$-S_1 + S_2 + \gamma m \delta - 2\gamma m x_2$
1028	+gradient	$S_1 + S_2 + \gamma m x_1$	$-S_1 + S_2 - \gamma m x_1$
1016	180 degree pulse	$-S_1 - S_2 - \gamma m x_1$	$S_1 - S_2 + \gamma m x_1$
1018	-gradient	$-S_1 - S_2 + \gamma m \delta - 2\gamma m_1 x_2$	$S_1 - S_2 - \gamma m \delta$
1020	$t_2/2$	$-S_1 + \gamma m \delta - 2\gamma m_1 x_2$	$S_1 - \gamma m \delta$
1022			Echo

While the echos are contaminated by S_1 , the S_2 contributions are cancelled. The procedure of Table 1 and FIG. 10 continues until limited by a transverse

relaxation time T_2 or other relaxation time. In the step 1022, the echo is associated with either the $+i\phi$ or $-i\phi$ phase terms and added to a corresponding image.

Simultaneous Dual-Echo Readout for STEAM

5 The readout scheme presented above has the advantage of utilizing the full extent of the available magnetization for collecting data by sampling either the STE or the STAE at any given acquisition window. In addition, it requires no special post-processing tools when compared to existing slower versions of DENSE. However, this scheme lacks the ability of simultaneously sampling both components 10 (STE and STAE) of the signal. By eliminating the second gradient encoding pulse (see FIG. 11B), both components can be sampled within the same acquisition window. The two components are separated in k-space by a distance of $2\gamma m_1 r_1$. Therefore, the acquisition window is extended to accommodate both components. Its actual duration will depend on the desired imaging parameters (such as field of 15 view ("FOV"), sampling speed, image resolution) and the encoding strength utilized. Since both components are rephased off-center within the acquisition period, a linear phase gradient will exist across the FOV of the image reconstructed from either component. In order to estimate this phase gradient and compensate for its effects via the image reconstruction algorithm, the gradient moment m_1 is preferably 20 compared to the area of the readout gradient pulse contained between two successive sampled points. Since this area of G_x/BW corresponds to a maximum of 2π phase evolution, the overall phase gradient across the FOV can be estimated and corrected for. However, in practice, hardware limitations can cause additional phase gradients across the FOV and therefore it is preferable to measure the phase gradient from an 25 immobile structure within the image, such as a representation of the liver margin, and adjust the correction factor accordingly. Once the phase gradient has been corrected in both images acquired from the two signal components (STE and STAE), the displacement information can be combined to yield a single dataset that possesses a higher signal-to-noise ratio. The resulting dataset will be contaminated 30 by the time varying phase terms, S_1 , by twice as much when compared to the STE alone.

Decoupling Overlapping STE and STAE in the Acquisition Window

In both acquisition schemes described above, it is assumed that the two echoes (STE and STAE) are separated in k-space adequately by means of the encoding gradient moment, m_1 , in order to avoid overlap of the two signal components. Such overlap can result in high-frequency content contamination during signal sampling and therefore diminished edge definition in the images. Unless such a penalty is acceptable, the two echoes are preferably separated by at least $\gamma N_x G_x / \text{BW}$, where N_x is the number of points along the x-direction. This translates to utilizing encoding gradient strengths (measured in mm/ π) of less than half the pixel size. This is true because the encoding gradient strength, Enc , is described by

$$Enc = \frac{1}{m_1 \cdot 2 \cdot 4250 \cdot 10^{-7}}$$

while the pixel size, p , is

$$p = \frac{1}{m_{READ} \cdot 4250 \cdot 10^{-7}}$$

15 and

$$m_1 \geq m_{READ}$$

With some encoding schemes, it is not always possible to utilize encoding pulses that will lead to such clear separation between the two components of the signal. A mechanism for distinguishing the two components in such cases is described below. For this description, it is assumed that the free induction decay (“FID”) has been suppressed.

For example, with the STEAM pulse sequence, the application of the gradient encoding pulse, with moment m_1 , results in imparting phase to the spins according to their position in space. As such, the net M_{XY} magnetization is 25 scrambled across the xy-plane on both the x and y-axes. As a result, the second 90° RF pulse can only nutate back to the longitudinal axis half of the signal, i.e., either M_x or M_y but not both. Since the total signal on the xy-plane is $M_{xy} = M_x + iM_y$, the phase of the second 90° pulse determines whether the real or the imaginary part of the signal is preserved for imaging later in the sequence. Assuming that a second

90° RF pulse along the same axis as the first preserves the real part, then one can write this portion of the magnetization as

$$M_x = \frac{M_x + iM_y}{2} + \frac{M_x - iM_y}{2} = \frac{1}{2}(M_{xy} + M_{xy}^*)$$

In other words, the real part of the signal can be described as the sum of the total signal plus its complex conjugate. Similarly, if a second experiment is carried out with the second RF pulse applied with a 90° phase relative to the first RF pulse then the imaginary part of the signal is preserved. This can be written as

$$M_y = i \cdot \frac{M_x + iM_y}{2} - i \cdot \frac{M_x - iM_y}{2} = \frac{i}{2}(M_{xy} - M_{xy}^*)$$

The imaginary part of the signal can be written as the difference between the total signal and its complex conjugate. By acquiring M_x and M_y by means of two measurements, the individual M_{xy} and M_{xy}^* , which correspond to the STE and STAE, respectively, can be decoupled from one another without the limits of the above equations. FID suppression can be accomplished as well by acquiring data from a third experiment with the phase of the third 90° pulse modified accordingly.

15

Rotating Wheel Method

In phase-labeled imaging, phase-labeled components of magnetization decay or lose coherence via several processes that are conventionally characterized by time constants T_1 , T_2 , and T_2^* . Many of the limitations imposed by these decay processes 20 can be overcome as follows, with a rotating wheel method illustrated in FIG. 13. Such a method permits voxel motion to be tracked at a series of times. For a magnetization that, at time t_1 , is phase-labeled so that

$$M_z = \{m(r)e^{i[f(r)-\phi]} - m(r)e^{-i[f(r)-\phi]}\}/(2i), M_{xy} = \{m(r)e^{i[f(r)-\phi]} + m(r)e^{-i[f(r)-\phi]}\}/2$$

and the initial coherence in M_{xy} is retained for a substantial period of time, both M_z and M_{xy} are used for data acquisition. Data is acquired at a series of time points t_n 25 after the initial phase labeling using a series of RF pulses and readout schemes that satisfies three conditions: (a) at each time point t_n , readout-induced phase dispersion in M_{xy} is refocused with gradient pulses before the next time point; (b) at some time points t_n , a portion of M_z is tipped onto the transverse plane to replenish 30 magnetization losses due to decay in M_{xy} due to various relaxation processes, while

a portion of the refocused M_{xy} is tipped into the longitudinal axis for storage; and (c) at least some adjacent RF pulses produce a nearly 180° flip, so that phase dispersion due to field inhomogeneities in B_0 are compensated, and the decay of the transverse component M_{xy} follows approximately the $1/T_2$ rate. When these three conditions

5 are satisfied, the phase-labeled transverse magnetization acquired at the time points decays at roughly the rate of $1/T_2$, while it is continuously or intermittently replenished by the labeled terms in the longitudinal magnetization that decay at the slower $1/T_1$ rate in most biological samples. An advantage of this method is that the labeled terms in M_{xy} are used to improve SNR, while the available acquisition time

10 is increased by continuously or intermittently storing part of M_{xy} on the longitudinal axis and replenishing M_{xy} with a portion of the phase-labeled magnetization M_z . By adjusting the RF pulse flip angles, the amount of M_z tipped into the transverse plane at each time point is controlled, and therefore the total time available for data acquisition is controlled. Generally, there exists a tradeoff between the data

15 acquisition time and the SNR at each time point, and one can choose a suitable balance between the two by adjusting the RF pulses, as well as how frequently M_z is tipped in the transverse plane to replenish M_{xy} .

In one example of phase labeling, the magnetizations of all voxels in a region of interest form spokes of a wheel in a plane perpendicular to the xy plane, after

20 phase labeling as shown in FIG. 12. The axis of the wheel is in the xy plane at an angle $\phi + \pi/2$ from the x axis. At time t_2 , a gradient-balanced RF pulse combination of flip angle α is applied along this direction (the direction perpendicular to the direction of the last 90° pulse in the phase labeling). This pulse turns the wheel around its axis by angle α as shown in FIG. 12, so that the longitudinal and

25 transverse magnetizations are

$$M_z = m(\mathbf{r}') \{ e^{i[f(\mathbf{r}') - \phi - \pi/2 - \alpha]} + m(\mathbf{r}) e^{-i[f(\mathbf{r}') - \phi - \pi/2 - \alpha]} \} / 2,$$

$$M_{xy} = m(\mathbf{r}') \{ e^{i[f(\mathbf{r}') - \phi - \alpha]} + m(\mathbf{r})^* e^{-i[f(\mathbf{r}') - \phi - \alpha]} \} / 2,$$

wherein $\mathbf{r}' = \mathbf{r}(t_1)$. One or more of the readout methods described above can be used to acquire M_{xy} and isolate the phase-label function $f(\mathbf{r}')$. All gradients used during

30 the readout period are rewound so that M_{xy} is restored to the form above.

At time t_3 , a gradient-balanced α RF pulse is applied along the direction $\phi + \pi/2$. The magnetizations are then:

$$M_z = m(r') \{ e^{i[f(r') - \phi - \pi/2 - 2\alpha]} + m(r) * e^{-i[f(r') - \phi - \pi/2 - 2\alpha]} \} / 2,$$

$$M_{xy} = m(r') \{ e^{i[f(r') - \phi - 2\alpha]} + m(r) * e^{-i[f(r') - \phi - 2\alpha]} \} / 2.$$

The readout and gradient rewinding process done at t_2 is performed again to acquire M_{xy} .

5 This process can be repeated for the series of time points: At each time t_n , an α RF pulse tips part of the longitudinal magnetization M_z onto the xy -plane and restores part of the M_{xy} along the z -axis. Mathematically, this is reflected as adding and subtracting α to the phases of the two terms in M_z and M_{xy} . FIG. 13 is a schematic diagram representation of such a pulse sequence, where the readout after 10 each α pulse is a gradient-recalled-echo readout. On average, the magnetization vector of a voxel spends equal times in the transverse plane and along the main field. Thus, the coherence of the magnetization decays at roughly half the rate of its 15 relaxation in the transverse plane (assuming the relaxation rate along the longitudinal direction is much lower). Because several consecutive α pulses approach a 180° RF pulse, any phase dispersion of the transverse magnetization due to B_0 inhomogeneity is refocused after several α pulses.

20 FIG. 13 illustrates one embodiment of the rotating-wheel acquisition method for mapping an x -component of the displacement at multiple time points. The phase-labeling segment consists of a 90° RF pulse followed by a gradient pulse, and then another 90° flip along the x -axis. This creates a spin wheel, with 25 $M_z = (e^{ikx} - e^{-ikx}) M_0 / (2i)$, $M_{xy} = (e^{ikx} + e^{-ikx}) M_0 / 2$. A fully balanced readout gradient is preferably applied to sample both terms of the transverse magnetization M_{xy} simultaneously, as represented by the two echoes above the readout period. The magnetization is returned to the above spin-wheel form after the balanced readout. Then, at time $t_1 + \Delta t$, an RF pulse of α flip angle is preferably applied around the y -axis, and the balanced readout is repeated. At time $t_1 + 2\Delta t$, this process is repeated again. During each readout period, the gradient waveforms are fully balanced (net time integral of the gradient waveforms is zero), so as not to add additional phase to the magnetization. This process is repeated for a series of time point $t_1 + n\Delta t$.

30 Each RF pulse in this sequence, including the 90° pulses in the phase-labeling section, are fully balanced so as not to leave residual phase dispersion on

the magnetization vectors, regardless of the initial orientation of the magnetization vector. A fully balanced slice-selective RF pulse 1302 in the form of a sinc function is illustrated in FIG. 13. The gradient area G under the slice-select gradient pulse is balanced by two gradient pulses of opposite sign and half the area ($G/2$), one applied immediately before the slice-select gradient pulse, the other immediately after the slice-select gradient pulse.

In biological samples, usually $T_1 \gg T_2$, so the MR signal in this method lasts approximately twice T_2 , during which the desired function $f(\mathbf{r}(t_n)) - f(\mathbf{r}(t_1))$ is repeatedly mapped to form a history of motion.

The RF pulses at the time points t_n need not have the same flip angle. As long as the flip angle for each pulse is known, the phase offsets brought about by the RF pulse to the terms in M_z and M_{xy} are known and preferably compensated for during image reconstruction. In cases where the flip angle is not exactly uniform in the region of interest, for example, with slice profile imperfections in slice-selective RF pulses, this flexibility allows several RF pulses to be used in one direction of spin rotation, and then an equal number of pulses in the other direction to compensate for the imperfections. In the pulse sequence of FIG. 13, this is implemented by replacing the series of α pulses with a series of $+\alpha$ and $-\alpha$ pulses, e.g., $(+\alpha, +\alpha, +\alpha, +\alpha, -\alpha, -\alpha, -\alpha, +\alpha, +\alpha, +\alpha, +\alpha, -\alpha, -\alpha, -\alpha, -\alpha, \dots)$.

This analysis leads to other embodiments in which the RF pulses for the time series alternate between $180^\circ - \alpha$ and $-(180^\circ - \alpha)$, α being a small angle (e.g., 30°). Since each RF flip is about 180° , it refocuses most of the phase dispersions in M_{xy} due to B_0 inhomogeneities. In the meantime, with each RF pulse a $1 - \cos(\alpha)$ portion of the longitudinal magnetization M_z is preferably brought into the transverse plane to replenish M_{xy} , while a $1 - \cos(\alpha)$ portion of the transverse magnetization M_{xy} is brought back to the z axis for storage. By reducing the angle α , the sustainable acquisition time approaches T_1 , while SNR at each time point is reduced. Raising α has the opposite effect.

In other embodiments, one can replace the α -pulse train in FIG. 13 with a repeating segment consisting of an even number of alternating 180° and -180° pulses followed by a small tip angle α pulse, i.e., $(180, -180, 180, -180, \alpha, 180, -180, 180, -180, \alpha, \dots)$. In each segment, the series of 180° pulses repeatedly refocus as the

transverse magnetization M_{xy} for readout, and then the α pulse tips a portion of the longitudinal magnetization into the transverse plane to replenish M_{xy} in preparation for data acquisition in the next segment.

Further embodiments include reading the transverse phase-encoded
5 magnetization with a train of 180-degree pulses, right after the phase label has been applied. The signal sampled during the series of 180-degree pulses can be used to form images, which possess phase-labeled information at different time points. The length of this readout period will be limited by T_2 relaxation. Once the transverse magnetization has decayed and is no longer useful for creating images, it is crushed
10 by gradient pulses. Following this, a 90-degree pulse can be utilized to bring the longitudinal magnetization onto the transverse plane. This part of the magnetization has experienced T_1 relaxation ($T_1 \gg T_2$) and, as such, has not decayed significantly. Imaging can now resume with a train of 180-degree pulses as mentioned above, to collect data from more time points.

15 There are many other possible embodiments of this general method in using a combination of other RF pulse series and readout schemes. If the RF pulses are slice selective, then the slice selective gradient needs to be fully balanced to avoid unwanted phase dispersion in the through-slice direction. FIG. 13 illustrates such a fully balanced slice selective pulse.

20 This method is called the rotating-wheel method because the magnetization vectors form a vertical wheel in the spin space after phase labeling, and the wheel rotates around its axis during data acquisition (See FIG. 12).

25 A cycling between imaging and storing magnetization along the z-axis can be maintained by applying a series of gradient-balanced 90° RF pulses. In this series, the phase of the 90° RF pulses can be changed by 180° after every four such pulses. By doing so, for every eight RF pulses, any deviations from a true 90° rotation are compensated for. In addition, both halves of the magnetization spend equal time along the longitudinal axis and the transverse plane. As a result they decay according to the same decay-rate, which is approximately two times T_2 . Field inhomogeneity is compensated for by the RF-train phase cycling scheme since the spins spend equal time along both positive and negative directions on the XY-plane.
30 Since for half the time the magnetization is protected from T_2 decay by storage

along the Z-axis, the decay rate due to spin-spin relaxation is $2T_2$. This is true only when $T_1 \gg T_2$, which is the case for non-contrast-enhanced specimens. For the portion of the magnetization being imaged, either one or both of the STE and STAE can be sampled as described previously. Since all RF pulses used are slice-selective, 5 through-plane motion may cause significant signal loss, especially for later acquisition windows. Increasing the slice-thickness of the pulses in the RF pulse series that follows the position-encoding gradient can provide slice tracking in order to avoid undesired signal loss. However, out-of-slice free induction decay (FID) contributions can degrade image quality. In cases of significant through-slice 10 motion, this problem can be solved by placing out-of-slice saturation pulses immediately before the position-encoding segment.

The acquisition methods can be adapted for mapping phase labels at a series of time points to track motion. At each time point after the initial phase labeling, a fraction of the longitudinal magnetization is tipped onto the transverse plane, and 15 data corresponding to the resulting transverse magnetization is acquired as described above. After data acquisition, the remaining transverse magnetization can be destroyed with gradient spoiler pulses, and this procedure repeated until the phase-labeled longitudinal magnetization is exhausted. To ensure that only a fraction of the phase-labeled longitudinal magnetization M_z is used each time, the tip angle of 20 the decoding RF-gradient waveform is preferably much less than 90° , e.g., 30° .

Free Induction Decay Suppression

FIG. 14 illustrates a DENSE measurement method. Referring to FIG. 14, during a time period TM between a second 90 degree pulse 1402 and a third 90 degree pulse 1404, the magnetization relaxes due to energy dissipation onto the 25 lattice according to T_1 to produce a contribution M_{FID} to the z-component of the magnetization. In the presence of an axial magnetic field B_0 that establishes an equilibrium +z-directed magnetization M_z (in the absence of RF pulses), a magnetization of magnitude $M_{initial} < M_z$ decays to form a z-component of magnetization $M(t)$, wherein $M(t) = M_z + (M_{initial} - M_z)exp(-t/T_1)$. 30 After a first 90 degree pulse 1406, the unlabeled transverse magnetization has a zero z-component so that $M_{FID} = M_z[1-exp(-\tau_1/T_1)]$ at a time τ_1 , wherein T_1 is a

longitudinal magnetization relaxation time. A 180 degree pulse 1404 flips M_{FID} to be directed along the $-z$ axis, i.e., $M_{FID} = -M_{FID}$. This flipped magnetization relaxes to produce a z -component of magnetization $M(\tau_2)$ at a selected time τ_2 and has a magnitude that can be determined by assigning $M_{initial}$ the value of M_{FID} so that

5 $M(\tau_2) = M_z + [-M_z(1 - \exp(-\tau_1/T_1)) - M_z] \exp(-\tau_2/T_1)$. The durations τ_1 and τ_2 can be selected so that at time τ_2 , $M(\tau_2) = 0$ by selecting $\tau_2 = T_1 \ln[2/(1 + \exp(-T_M/T_1))]$. As a representative example, for a mixing time $T_M = 300$ ms and a longitudinal relaxation time $T_1 = 300$ ms, $\tau_1 = 262.2$ ms and $\tau_2 = 138.8$ ms.

10 Selection of τ_1 and τ_2 for FID suppression depends on the longitudinal relaxation time T_1 and because T_1 is generally material dependent. For example, for myocardial tissue T_1 is approximately 850 ms while for fat tissue, T_1 is approximately 200 ms. However, FID associated with two time constants can be suppressed by providing an additional 180 degree pulse and corresponding time intervals.

15

Reduction of Phase Errors by Interleaved Data Acquisition

Phase-labeled terms acquired during readout contain the phase-label function as well as other additional phase contributions from eddy currents, B_0 inhomogeneities, etc.. These contributions bring errors into the measurement. One 20 method of removing these phase errors is to acquire two data sets that are phase-labeled with different functions, $af(r)$ and $bf(r)$, where a and b are different constants. These two data sets share the same unknown phase contributions. By subtracting their respective results, we obtain $(a-b)[f(r')-f(r)]$, and the common phase errors are removed. These two data sets can be acquired under the same 25 condition of motion, preferably in an interleaved fashion, to reduce errors from small changes in the position and movement of the object.

Resolving Phase Ambiguities

The phase of an MRI signal is normally expressed in the range of 0 to 2π radians. When a specified phase-label function exceeds this range, the acquired 30 phase-label distribution contains step-like jumps of 2π magnitude. This phenomenon is called "phase wrap-around." Phase wrap-around is corrected by first

locating the discontinuous boundaries where this jump occurs, and then, for each boundary, the phase of the voxels on one side of the boundary is added or subtracted with an integer multiple of 2π , such that the discontinuity is removed. This procedure is generally effective. In some specimens, a bulk motion of an isolated region needs to be measured in relation to other regions and phase differences between these regions are ambiguous. In diagnostic imaging, the purpose of motion tracking is usually to characterize the internal movements of a contiguous area, where phase unwrapping is sufficient to resolve the ambiguity. In certain applications, measurements of local tissue deformation are needed, such as the strain in the myocardium. For these applications, it is not necessary to unwrap the phase for the entire region of interest as a whole, but rather it is sufficient to phase-unwrap each small area encompassing a group of neighboring voxels, and obtain the local deformation in this area.

Strain Data Display

15 In certain applications of MRI motion tracking, it is advantageous to quantify the deformation of a region by computing material strain. An example is strain mapping in the myocardium. In a two-dimensional (2D) plane, such as a 2D image through the long axis of the left ventricle, strain tensor maps can be calculated once the in-plane components of displacement vectors are mapped with one or more of
20 the methods described in the previous sections. The strain tensor at each voxel is represented by the strain values (negative for compression and positive for stretching) along two orthogonal directions, called principal axes of strain. Both the strain values and the principal axes contain useful information in many cases. The strain values can be display using short, thick line segments of uniform length to
25 represent the principal axes at each voxel, while the a color or a grayscale intensity of the line segments represent the strain values. The strain data can be presented in two strain images, each containing strain values of a particular sign, so that one map presents the axes and strain values for compression, while the other presents the axes and strain values for stretching. The color or grayscale intensity in each map
30 represents the absolute value of the positive or negative strain. If a voxel has the

same sign of strain for both principal axes, then in one map, two orthogonal line segments appear in its position, while in the other map the line segments are absent.

Alternatively, the strain data can be separated into two maps containing the higher and lower strain values, respectively. Then, each voxel in a map contains one line segment, whose color or grayscale intensity represents the corresponding strain value. Since each map may contain both positive and negative strain values, the color scale or gray intensity scale may need to represent a range of values from negative to positive, and a mixture of color and gray-intensity scale can be used for this purpose.

Strain data can also be displayed in a single image by providing each voxel with orthogonal line segments of uniform length to represent the principal axes of strain. The color or grayscale intensity of each line segment represents the corresponding strain value. A mixture of color scale and gray intensity scale can be used to cover a range of values including both negative and positive numbers.

Example embodiments of the invention are described above. It will be appreciated that these embodiments can be modified in arrangement and detail without departing from the scope of the invention.

63198-1362

CLAIMS:

1. A magnetic resonance imaging method, comprising:
 - applying a first excitation radio-frequency (RF) pulse along a first excitation axis to produce a first transverse magnetization;
 - applying a first position encoding phase label to the first transverse magnetization;
 - storing a component of the position encoded first transverse magnetization as a first stored longitudinal magnetization by applying a first storing RF pulse along a first storing axis;
 - allowing a first mixing time interval of duration T_M to elapse;
 - after the first mixing time has elapsed, producing a transverse magnetization based on the first stored longitudinal magnetization;
 - decoding the transverse magnetization produced after the first mixing time;
 - generating a first image signal based on the decoded transverse magnetization produced after the first mixing time;
 - applying a second excitation RF pulse along a second excitation axis to produce a second transverse magnetization;
 - 25 applying a second position encoding phase label to the second transverse magnetization;

63198-1362

34

storing a component of the position encoded second transverse magnetization as a second stored longitudinal magnetization by applying a second storing RF pulse along a second storing axis, wherein a difference between an angle 5 from the first excitation axis to the first storing axis and an angle from the second excitation axis to the second storing axis is not an integer multiple of 180 degrees;

allowing a second mixing time of duration T_M to elapse;

10 after the second mixing time has elapsed, producing a transverse magnetization based on the second stored longitudinal magnetization;

decoding the transverse magnetization produced after the second mixing time;

15 generating a second image signal based on the decoded transverse magnetization produced after the second mixing time; and

20 combining the first image signal and the second image signal to reduce a contribution associated with a complex conjugate of a phase-labeled magnetization to obtain an artifact-reduced image of a specimen.

2. The method of claim 1, further comprising estimating specimen motion based on the combined first image signal and second image signal.

25 3. The method of claim 2, wherein the first excitation axis and the first storing axis are orthogonal.

4. The method of claim 2, further comprising:

dividing the mixing time intervals of duration T_M into a first interval of duration t_1 and a second interval of

63198-1362

35

duration t_2 , where the first and second intervals are selected based on at least one longitudinal decay time T_1 ; and

5 applying a 180° radio-frequency (RF) pulse to the specimen after the time interval t_1 during acquisition of both the first image signal and the second image signal to reduce contributions associated with free induction decay.

5. The method of claim 4, wherein time points within the mixing time intervals divide the mixing time intervals 10 into a first interval of duration t_1 and a second interval of duration t_2 such that $t_2=\ln[2/(1+\exp(-T_M/T_1))]$, wherein T_1 is a longitudinal decay time and $T_M=t_1+t_2$.

6. The method of claim 2, further comprising applying RF pulses to the specimen at time points within the mixing 15 time intervals, wherein the time points are selected to reduce a contribution to the image signals from free induction decay.

7. The method of claim 1, wherein the first and second position encoding phase labels are applied along a 20 selected displacement direction.

8. The method of claim 7, further comprising estimating specimen motion based on the combined first image signal and second image signal.

9. The method of claim 8, wherein the first 25 excitation axis and the first storing axis are orthogonal.

10. The method of claim 8, further comprising:

dividing the mixing time intervals of duration T_M into a first interval of duration t_1 and a second interval of duration t_2 , wherein the first and second intervals are

63198-1362

selected based on at least one longitudinal decay time T_1 ;
and

applying a 180° radio-frequency (RF) pulse to the specimen after the time interval t_1 during acquisition of
5 both the first image signal and the second image signal to reduce contributions associated with free induction decay.

11. The method of claim 8, wherein time points within the mixing time intervals divide the mixing time intervals into a first interval of duration t_1 and a second interval of
10 duration t_2 such that $t_2 = \ln[2/(1+\exp(-T_M/T_1))]$, wherein T_1 is a longitudinal decay time and $T_M = t_1 + t_2$.

12. The method of claim 8, further comprising applying RF pulses to the specimen at time points within the mixing time intervals, wherein the time points are selected to
15 reduce a contribution to the image signals from free induction decay.

13. A magnetic resonance imaging method, comprising:

applying a first excitation radio-frequency (RF) pulse along a first excitation axis to produce a first
20 transverse magnetization;

applying a first position encoding phase label to the first transverse magnetization;

25 storing a component of the position encoded first transverse magnetization as a first stored longitudinal magnetization by applying a first storing RF pulse along a first storing axis;

allowing a first mixing time interval of duration T_M to elapse;

63198-1362

37

after the first mixing time has elapsed, producing a transverse magnetization based on the first stored longitudinal magnetization;

5 decoding the transverse magnetization produced after the first mixing time;

generating a first image signal based on the decoded transverse magnetization produced after the first mixing time;

10 applying a second excitation RF pulse along a second excitation axis to produce a second transverse magnetization;

applying a second position encoding phase label to the second transverse magnetization;

15 storing a component of the position encoded second transverse magnetization as a second stored longitudinal magnetization by applying a second storing RF pulse along a second storing axis;

allowing a second mixing time of duration T_M to elapse;

20 after the second mixing time has elapsed, producing a transverse magnetization based on the second stored longitudinal magnetization;

decoding the transverse magnetization produced after the second mixing time;

25 generating a second image signal based on the decoded transverse magnetization produced after the second mixing time;

· 63198-1362

applying a third excitation RF pulse along a third excitation axis to produce a third transverse magnetization;

applying a third position encoding phase label to the third transverse magnetization;

5 storing a component of the position encoded third transverse magnetization as a third stored longitudinal magnetization by applying a third storing RF pulse along a third storing axis, wherein an angle from the first excitation axis to the first storing axis, an angle from the 10 second excitation axis to the second storing axis, and an angle from the third excitation axis to the third storing axis are different;

allowing a third mixing time interval of duration T_M to elapse;

15 after the third mixing time has elapsed, producing a transverse magnetization based on the third stored longitudinal magnetization;

decoding the transverse magnetization produced after the third mixing time;

20 generating a third image signal based on the decoded transverse magnetization produced after the third mixing time; and

25 combining the first, second, and third image signals to reduce either a contribution associated with a complex conjugate of a phase-labeled magnetization or free induction decay, or both to obtain an artifact-reduced image of a specimen.

63198-1362

39

14. The method of claim 13, further comprising estimating specimen motion based on the combined first, second, and third image signals.

15. The method of claim 14, further comprising:

5 dividing the mixing time intervals into a first interval of duration t_1 and a second interval of duration t_2 , wherein the first and second intervals are selected based on at least one longitudinal decay time T_1 ; and

10 applying a 180° radio-frequency (RF) pulse to the specimen after the time interval t_1 during acquisition of the image signals to reduce contributions associated with free induction decay.

16. The method of claim 15, wherein the first interval of duration t_1 and the second interval of duration t_2 are 15 selected such that $t_2=T_1 \ln[2/(1+\exp(-T_M/T_1))]$, and $T_M=t_1+t_2$.

17. The method of claim 14, further comprising applying radio-frequency (RF) pulses to the specimen at time points within the mixing time intervals, wherein the time points are selected to reduce contributions to the image 20 signals from free induction decay.

18. The method of claim 13, wherein the first, second, and third position encoding phase labels are applied along a selected displacement direction.

19. The method of claim 18, further comprising 25 estimating specimen motion based on the combined first, second, and third image signals.

20. The method of claim 19, further comprising:

dividing the mixing time intervals into a first interval of duration t_1 and a second interval of duration t_2 ,

• 63198-1362

40

wherein the first and second intervals are selected based on at least one longitudinal decay time T_1 ; and

5 applying a 180° radio-frequency (RF) pulse to the specimen after the time interval t_1 during acquisition of the image signals to reduce contributions associated with free induction decay.

21. The method of claim 20, wherein the first interval of duration t_1 and the second interval of duration t_2 are selected such that $t_2=T_1 \ln[2/(1+\exp(-T_M/T_1))]$, and $T_M=t_1+t_2$.

10 22. The method of claim 19, further comprising applying radio-frequency (RF) pulses to the specimen at time points within the mixing time intervals, wherein the time points are selected to reduce contributions to the image signals from free induction decay.

15 23. A magnetic resonance imaging method, comprising:

applying an excitation radio-frequency (RF) pulse along an excitation axis to produce a transverse magnetization;

20 applying a position encoding phase label to the transverse magnetization;

storing a component of the position encoded transverse magnetization as a stored longitudinal magnetization by applying a storing RF pulse along a storing axis;

25 allowing a mixing time interval of duration T_M to elapse;

applying an RF pulse at a time point within the mixing time interval, wherein the time point is selected to reduce a signal contribution from free induction decay;

63198-1362

41

after the first mixing time has elapsed, producing a transverse magnetization based on the stored longitudinal magnetization;

decoding the transverse magnetization produced
5 after the mixing time;

generating an image signal of a specimen and producing an associated image of the specimen based on the decoded transverse magnetization produced after the mixing time.

10 24. The method of claim 23, further comprising estimating specimen motion based on the generated image signal.

25. The method of claim 24, further comprising:

dividing the mixing time interval into a first
15 interval of duration t_1 and a second interval of duration t_2 , wherein the first and second intervals are selected based on at least one longitudinal decay time T_1 ; and

applying a 180° radio-frequency (RF) pulse to the specimen after the time interval t_1 .

20 26. The method of claim 25, wherein the time point within the mixing time interval divides the mixing time interval into a first interval of duration t_1 and a second interval of duration t_2 such that $t_2=\ln[2/(1+\exp(-T_M/T_1))]$, wherein T_1 is a longitudinal decay time and $T_M=t_1+t_2$.

25 27. The method of claim 23, wherein the position encoding phase label is applied along a selected displacement direction.

• 63198-1362

42

28. The method of claim 27, further comprising estimating specimen motion based on the generated image signal.

29. The method of claim 28, further comprising:

5 dividing the mixing time interval into a first interval of duration t_1 and a second interval of duration t_2 , wherein the first and second intervals are selected based on at least one longitudinal decay time T_1 ; and

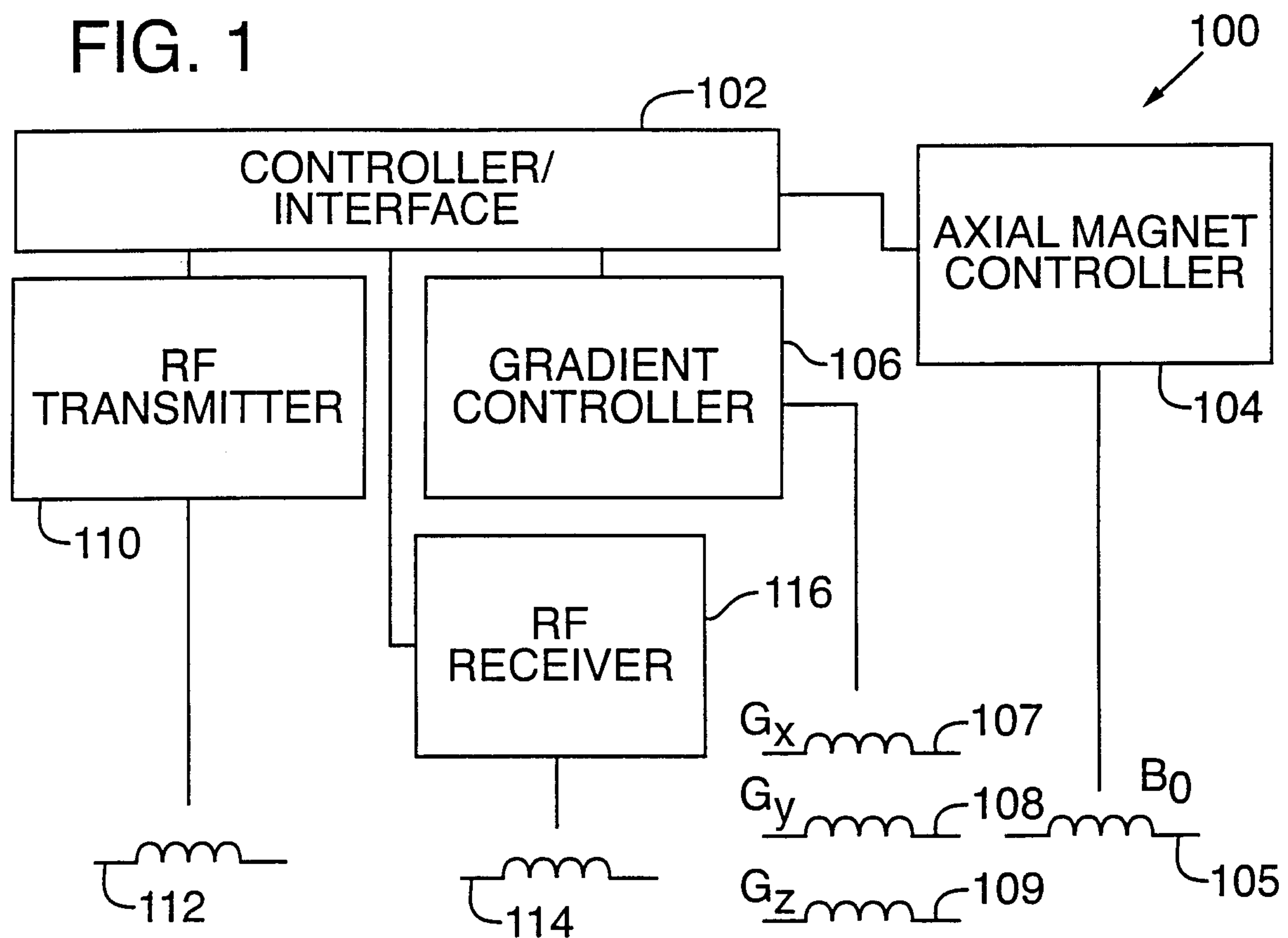
10 applying a 180° radio-frequency (RF) pulse to the specimen after the time interval t_1 .

30. The method of claim 29, wherein the time point within the mixing time interval divides the mixing time interval into a first interval of duration t_1 and a second interval of duration t_2 such that $t_2=\ln[2/(1+\exp(-T_M/T_1))]$,
15 wherein T_1 is a longitudinal decay time and $T_M=t_1+t_2$.

SMART & BIGGAR
PATENT AGENTS
OTTAWA, ONTARIO

1/9

FIG. 1



2/9

FIG. 2A

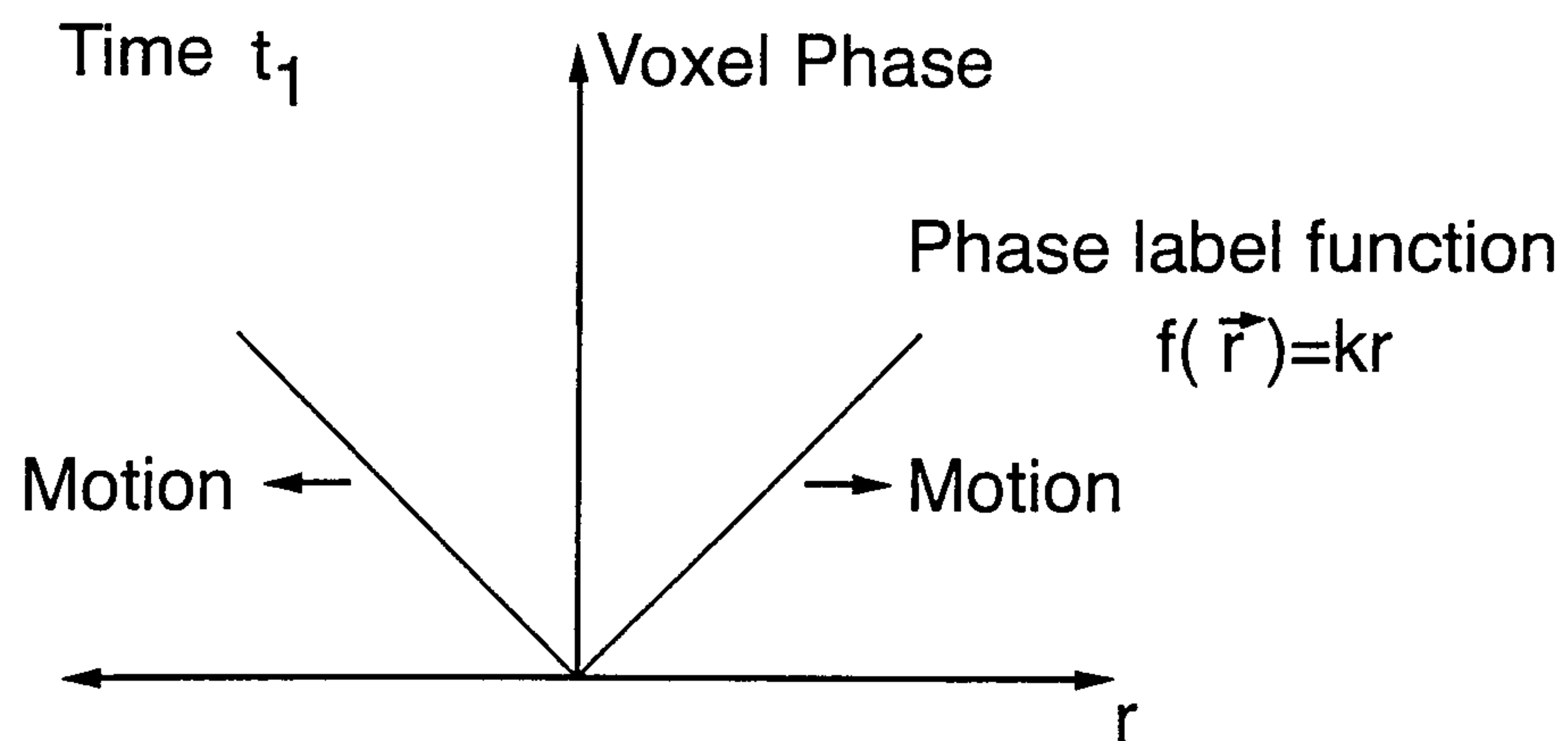
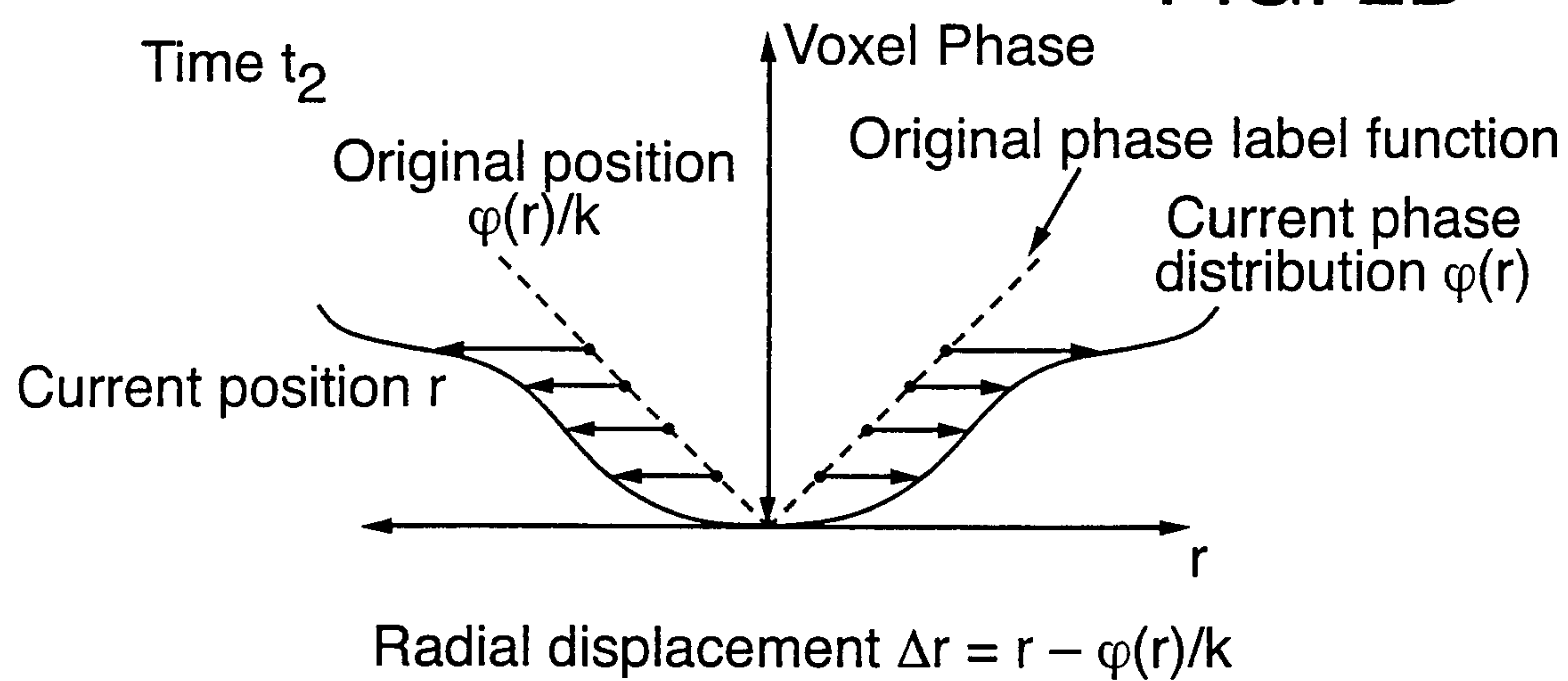


FIG. 2B



3/9

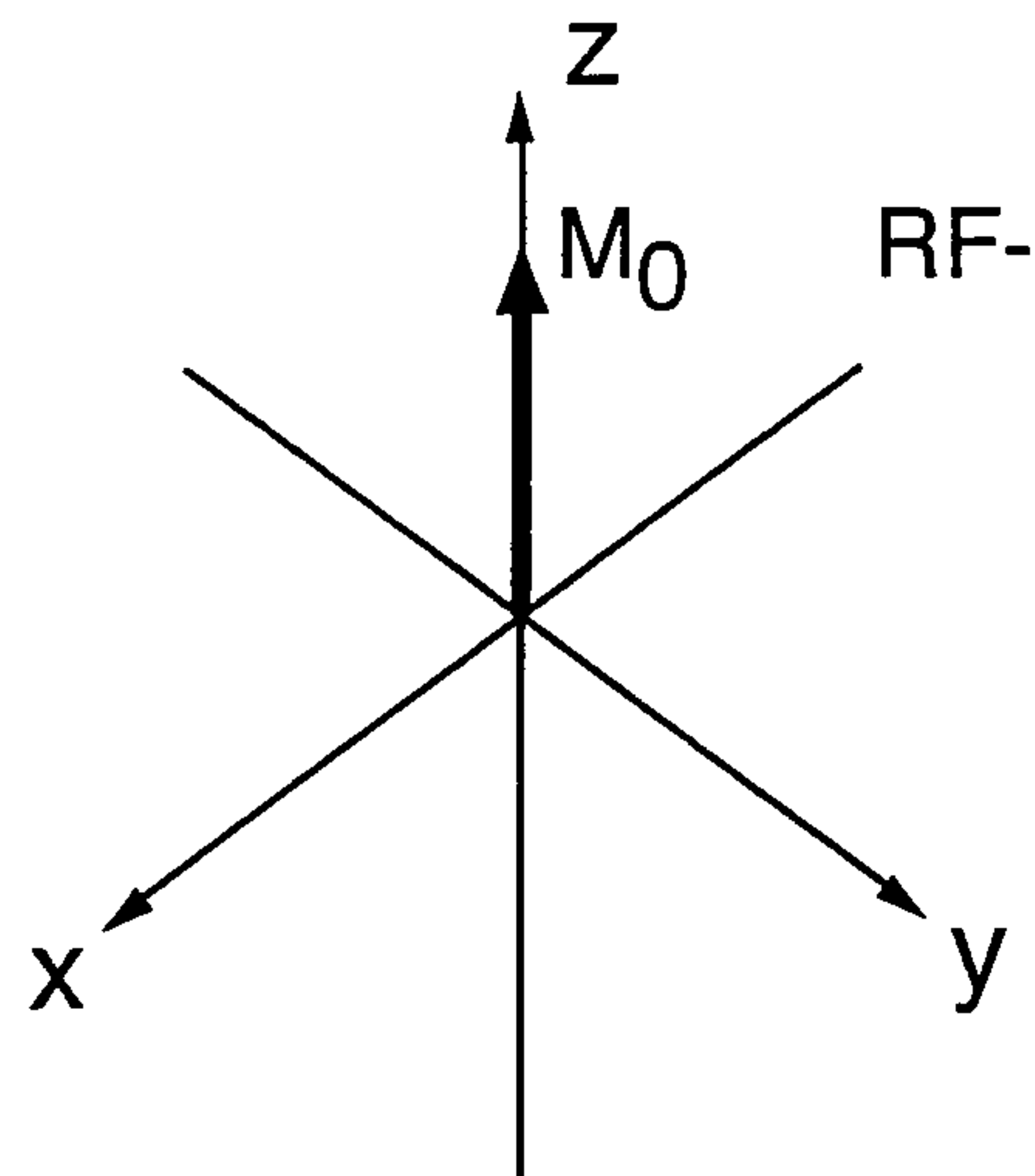


FIG. 3A

RF-gradient waveform

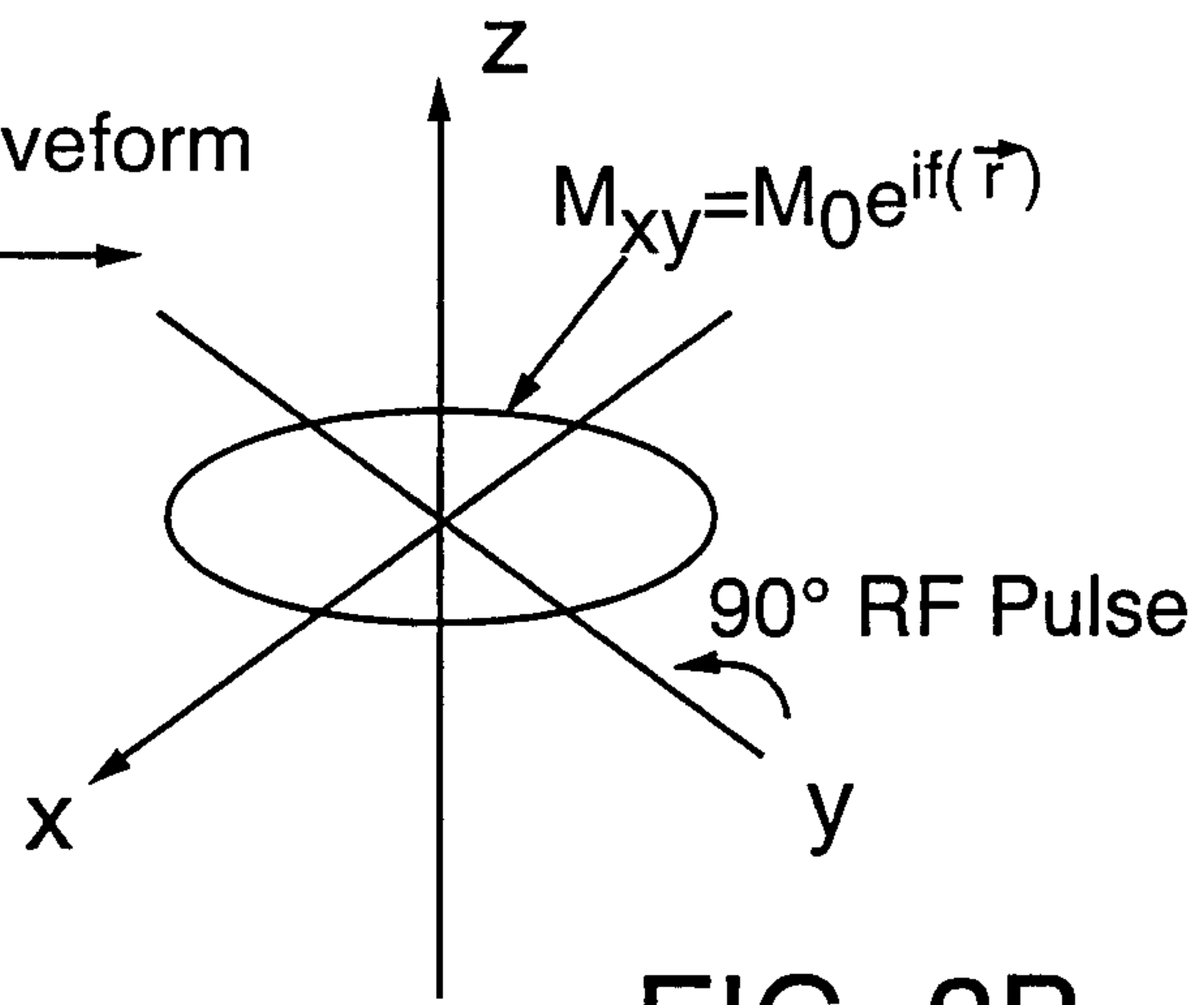


FIG. 3B

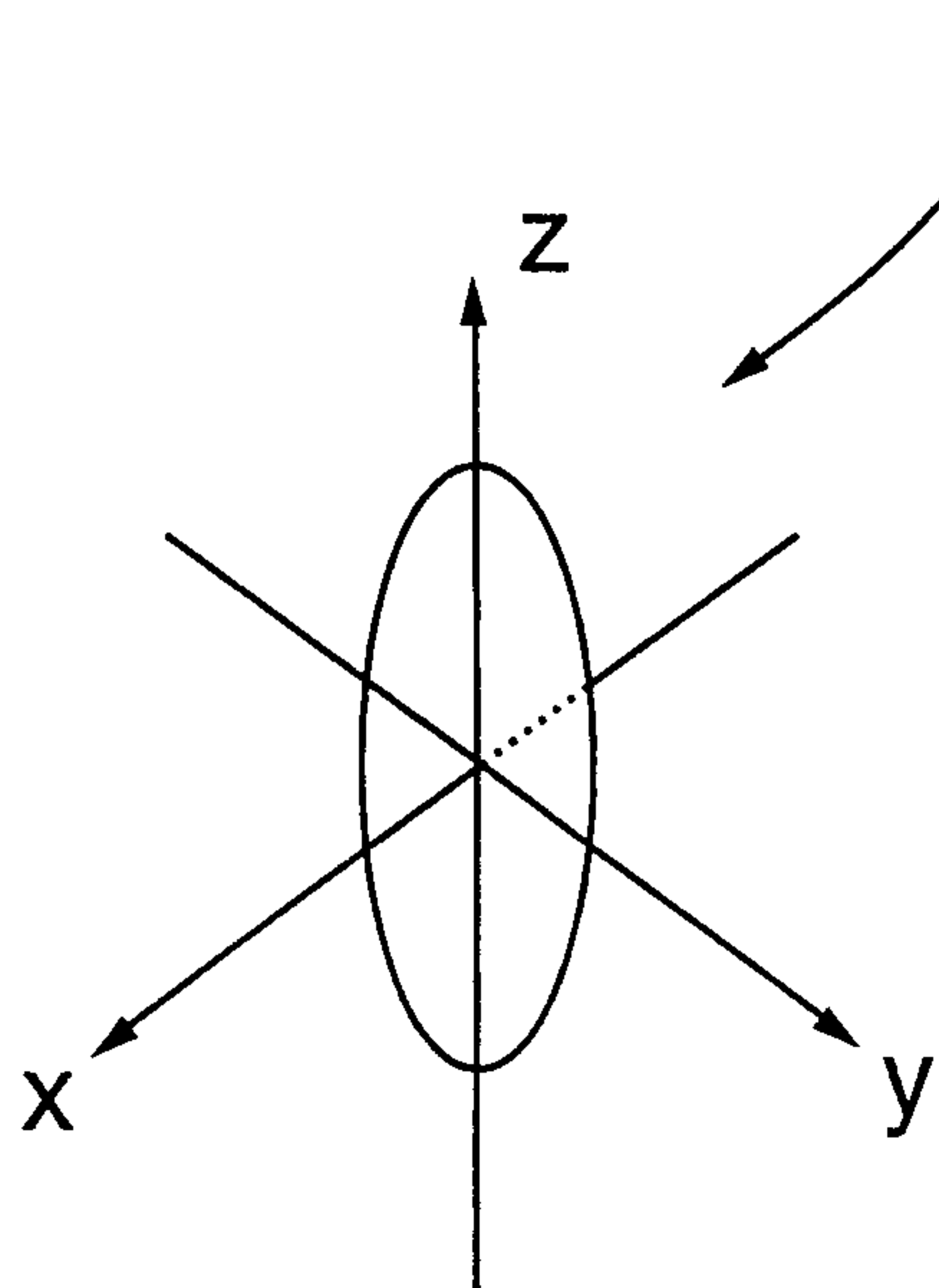


FIG. 3C

$$M_z = \frac{M_0}{2} (e^{if(r)} + e^{-if(r)})$$

$$M_{xy} = \frac{M_0}{2i} (e^{if(r)} - e^{-if(r)})$$

4/9

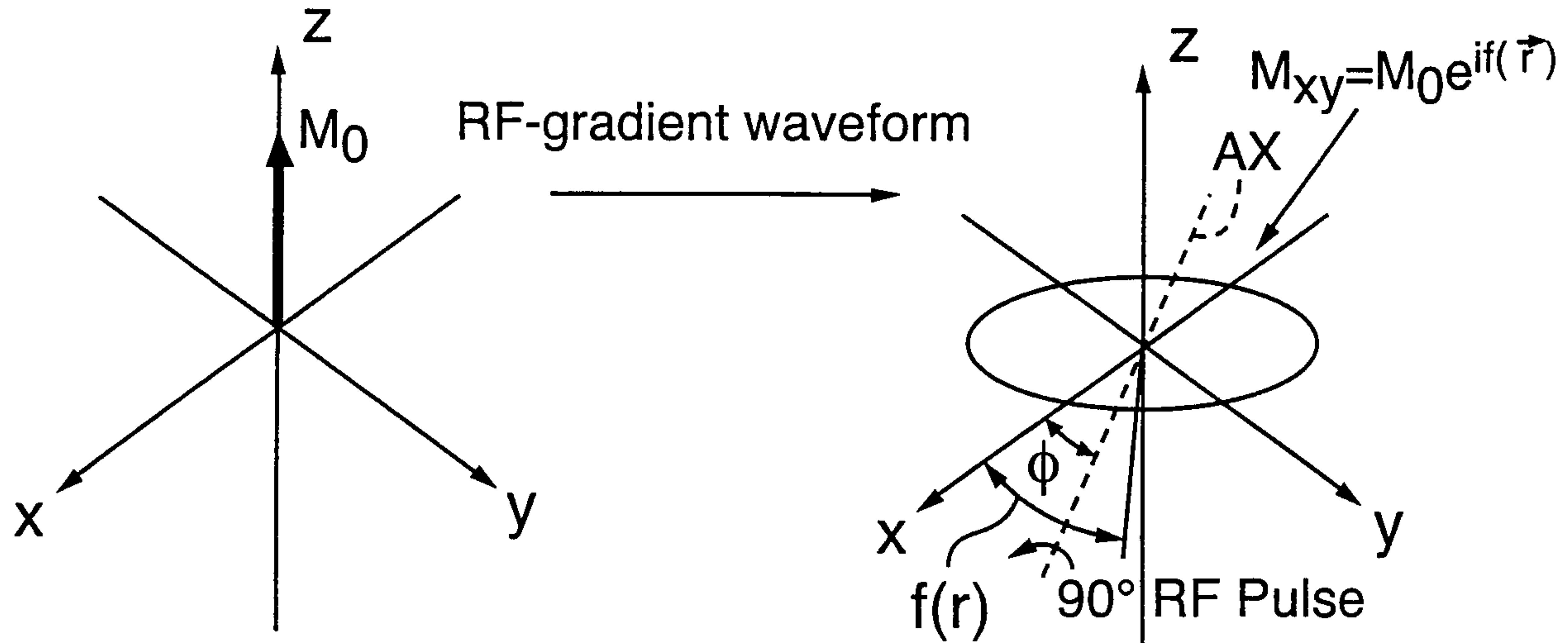
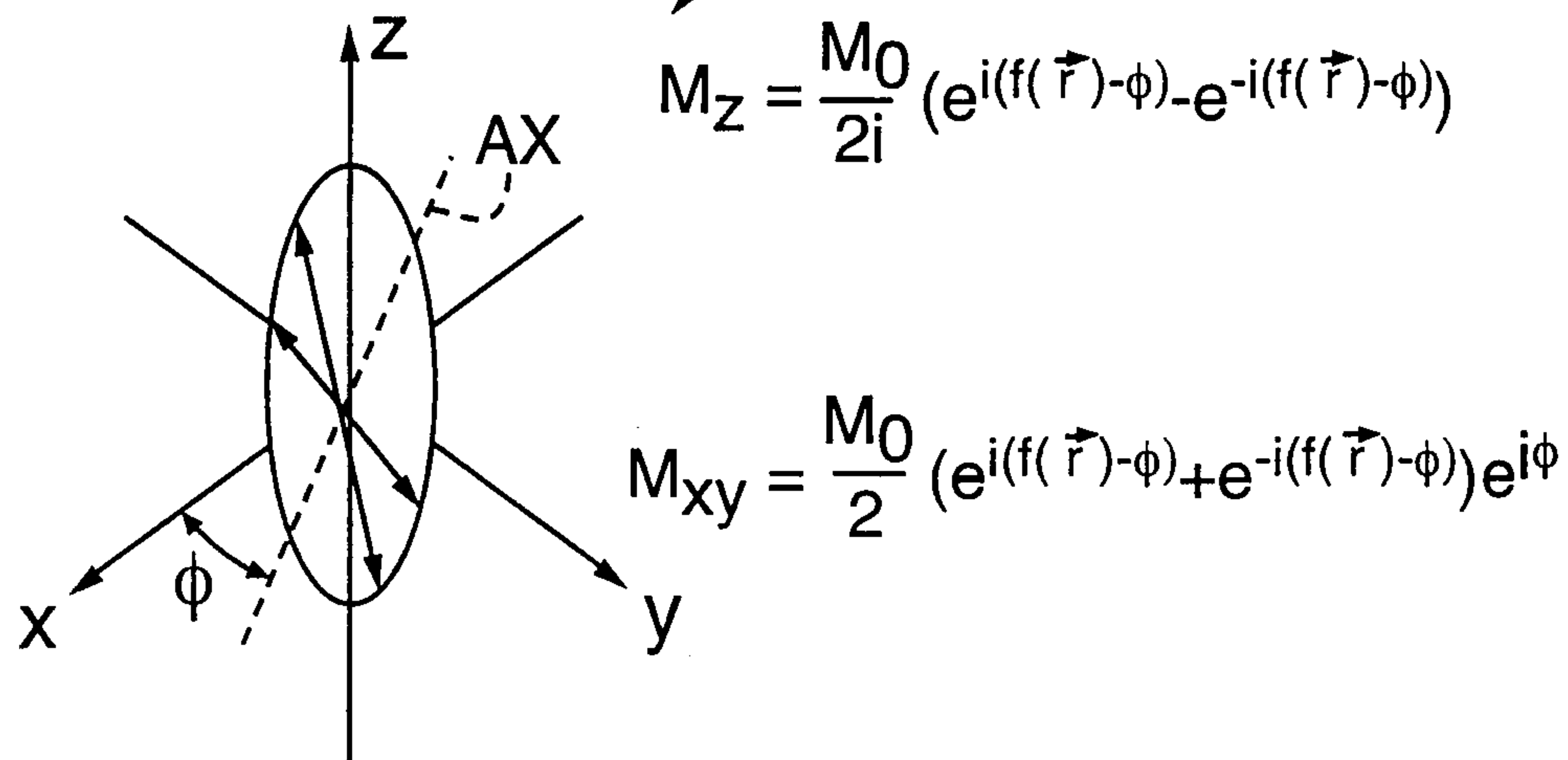


FIG. 4B

$$M_{xy} = M_0 e^{if(\vec{r})}$$



$$M_z = \frac{M_0}{2i} (e^{i(f(\vec{r})-\phi)} - e^{-i(f(\vec{r})-\phi)})$$

5/9

FIG. 5

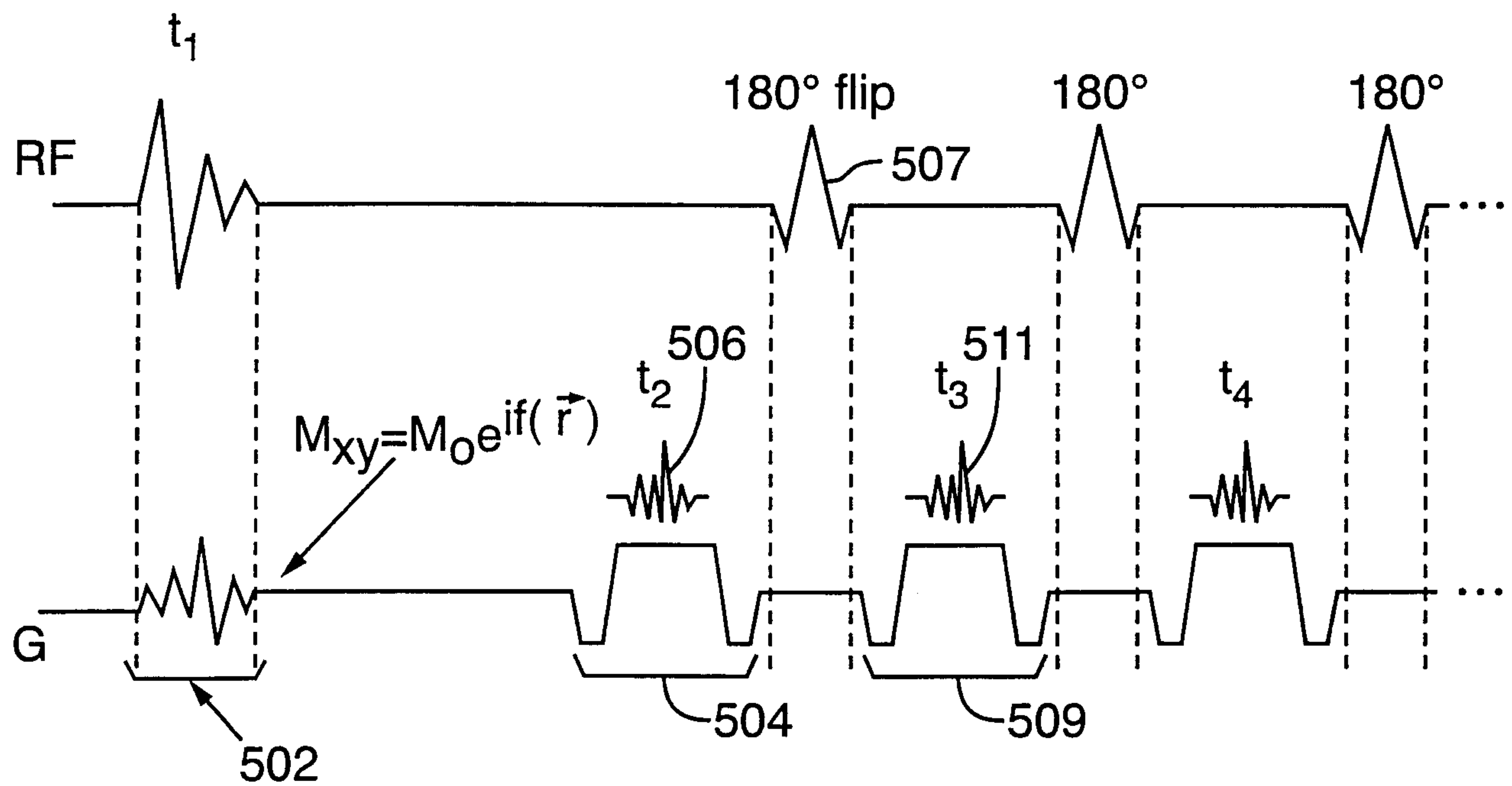
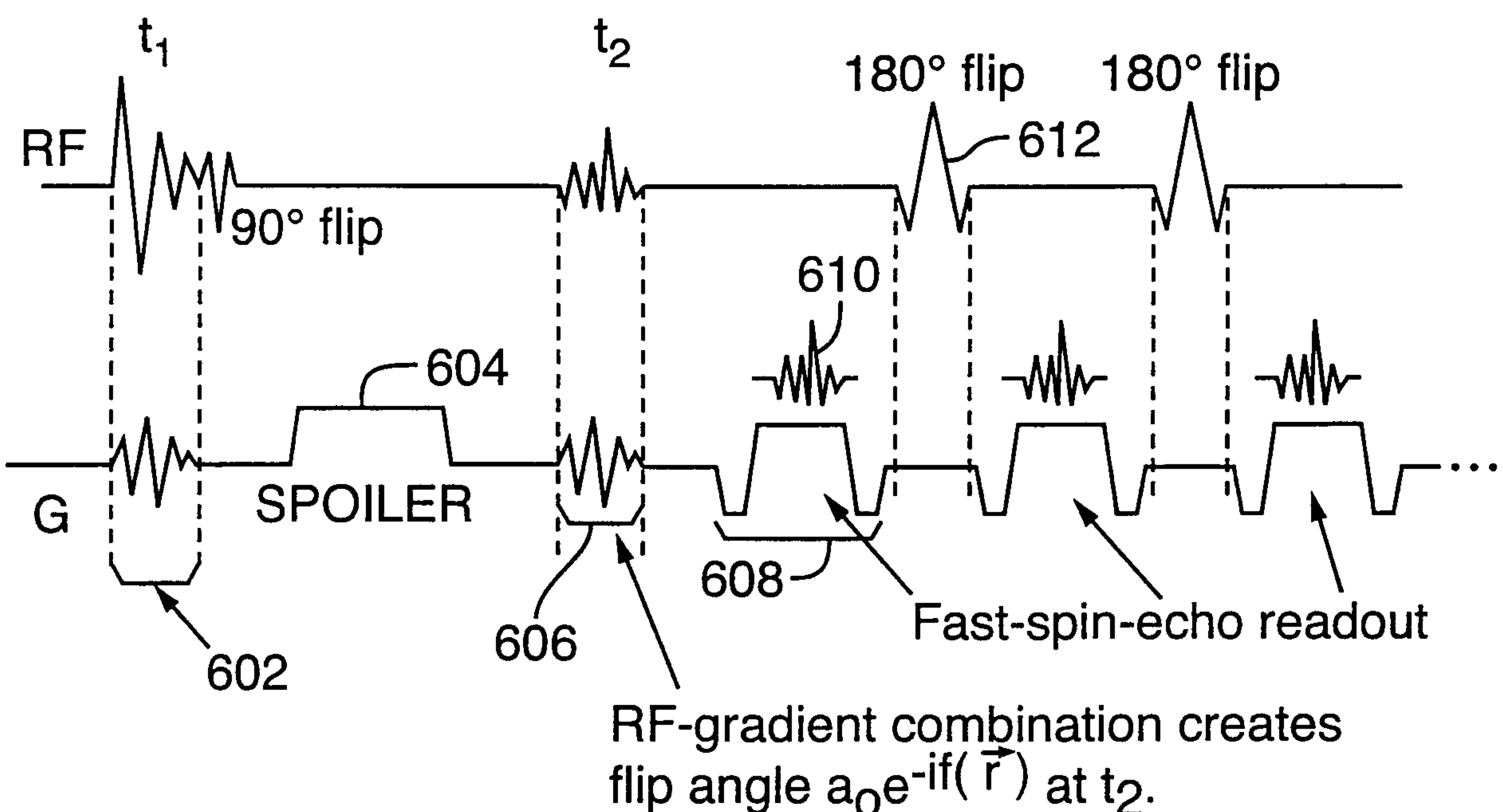


FIG. 6



6/9

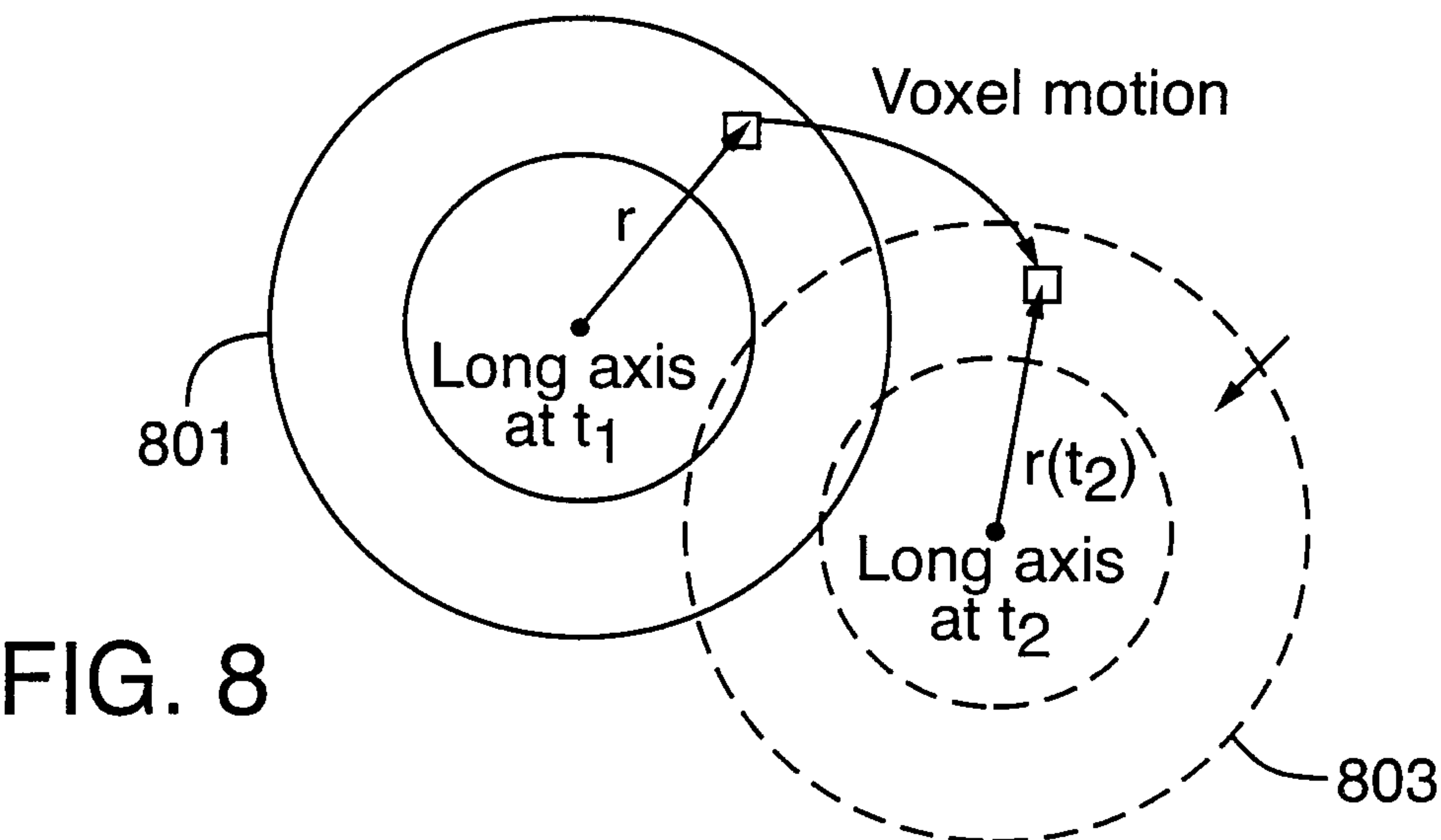
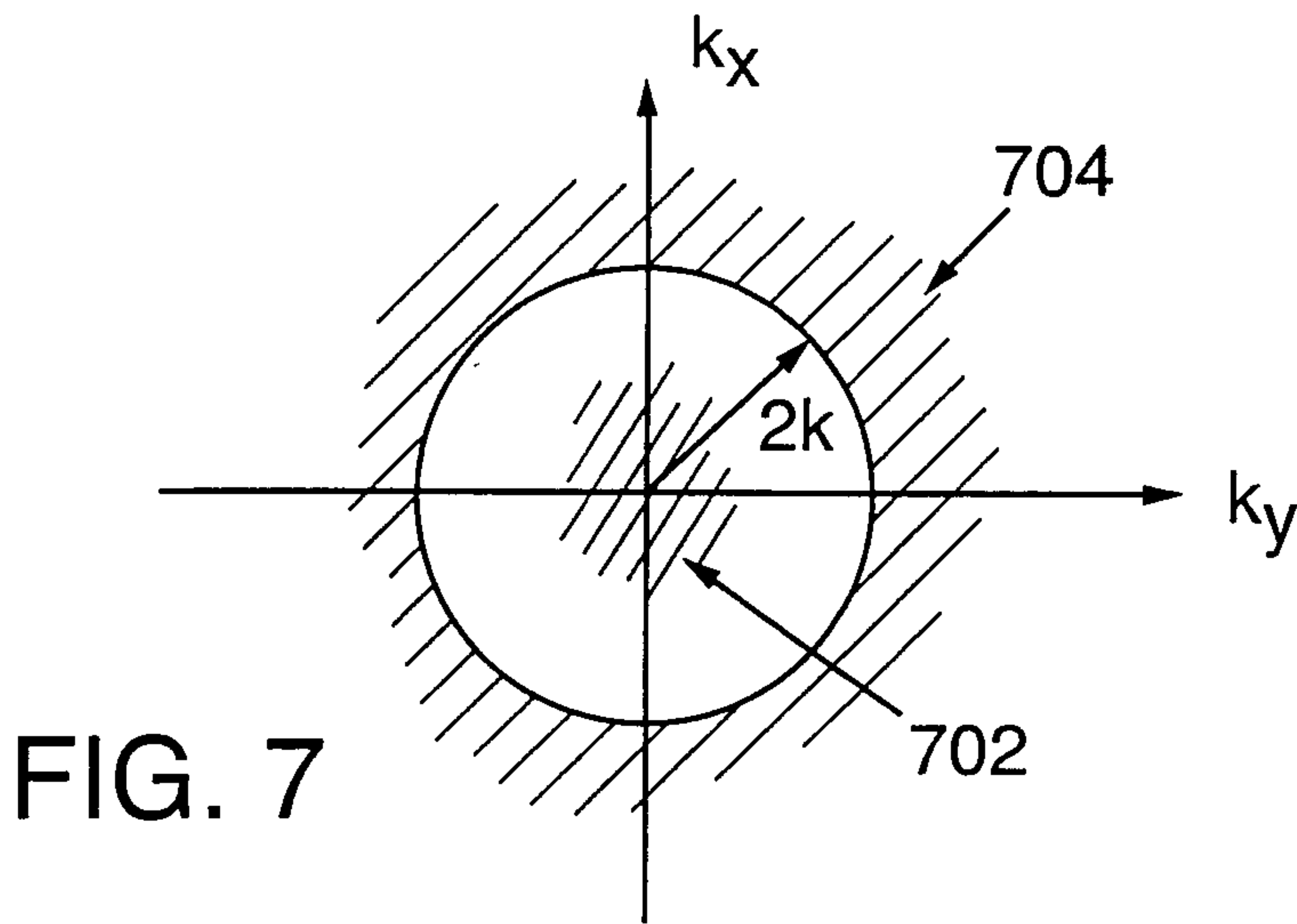
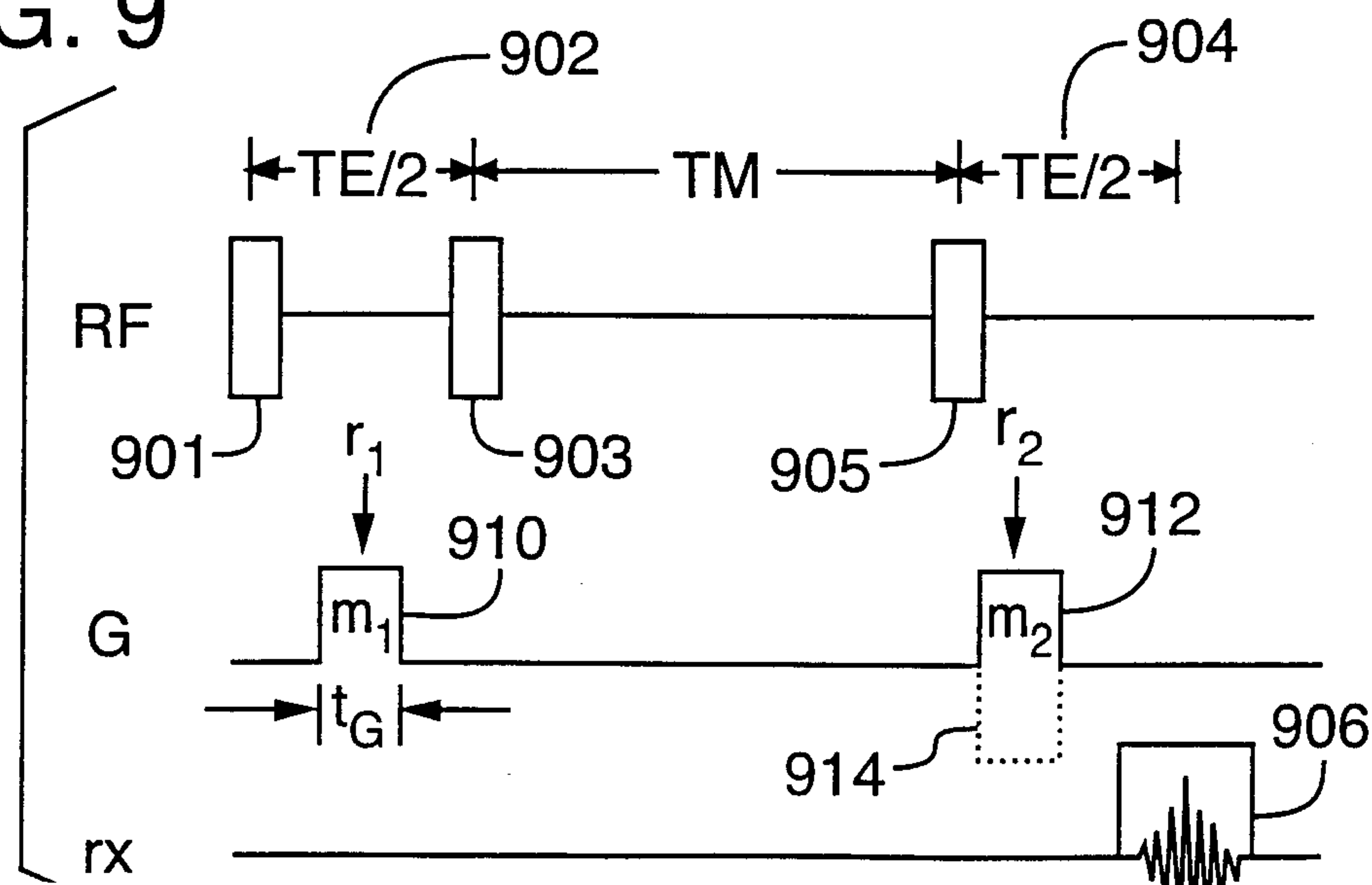
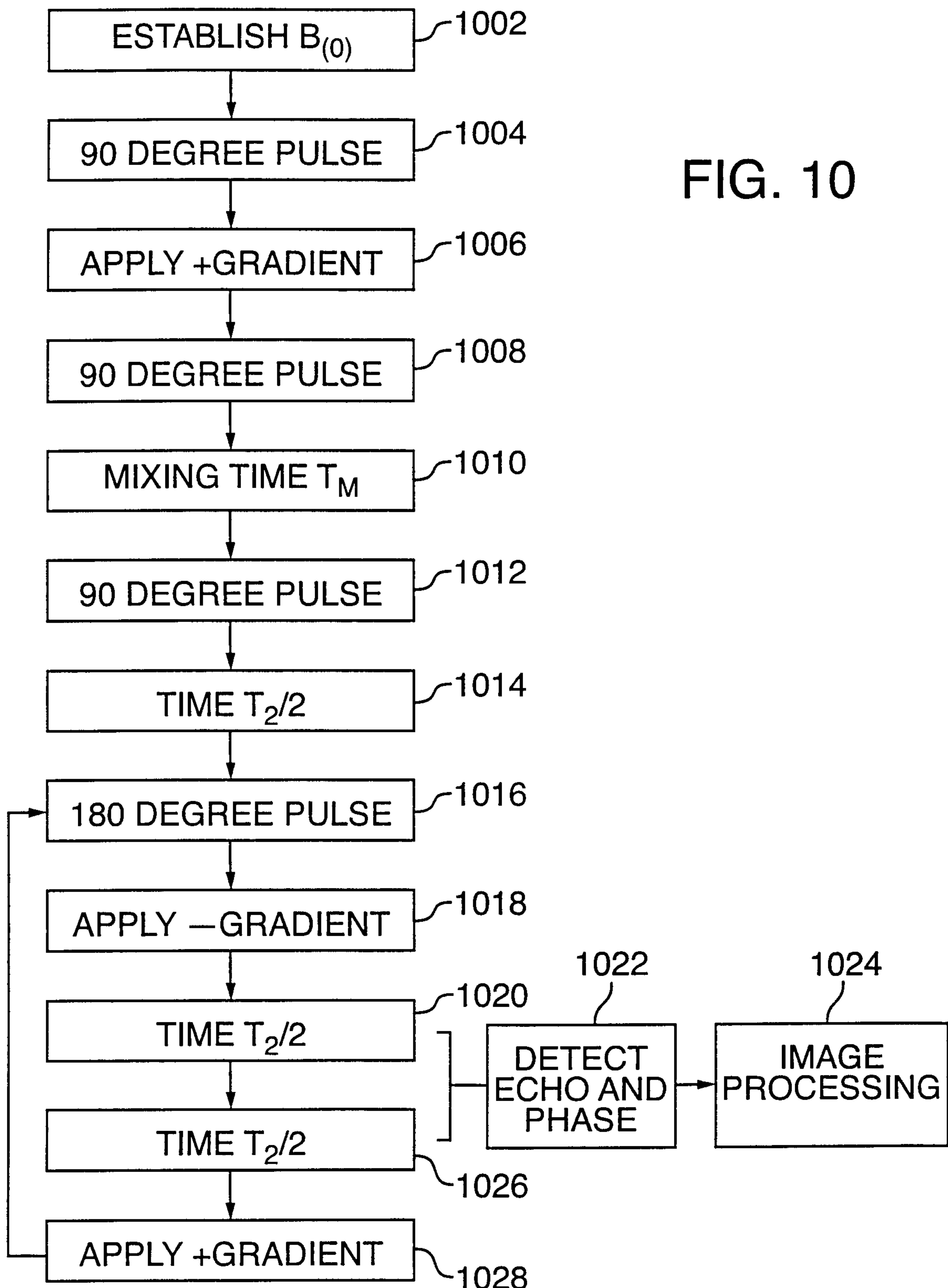


FIG. 9



7/9



8/9

FIG. 11A

$$M_{xy} = M_0 e^{i\phi(\vec{r})}$$

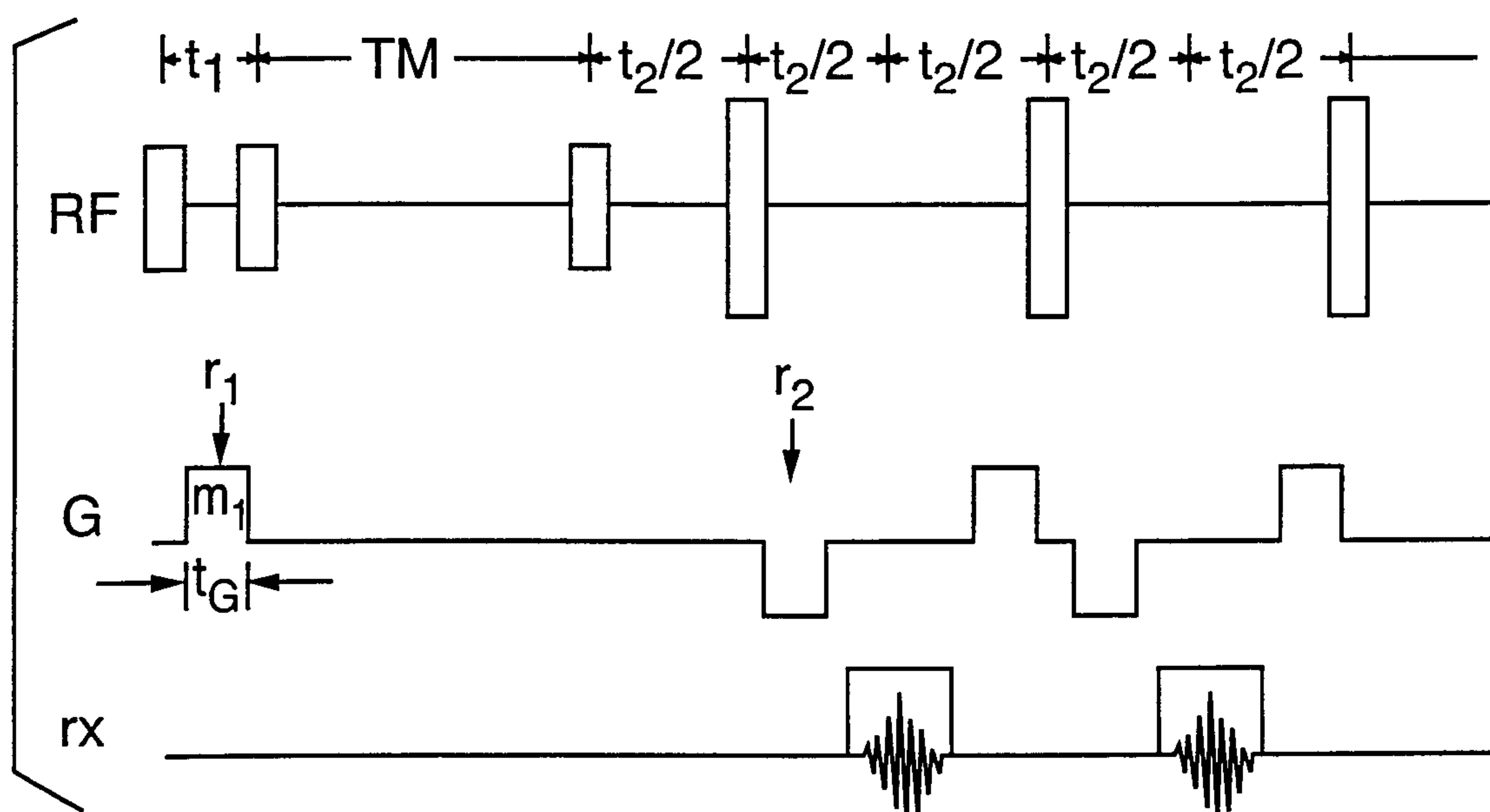
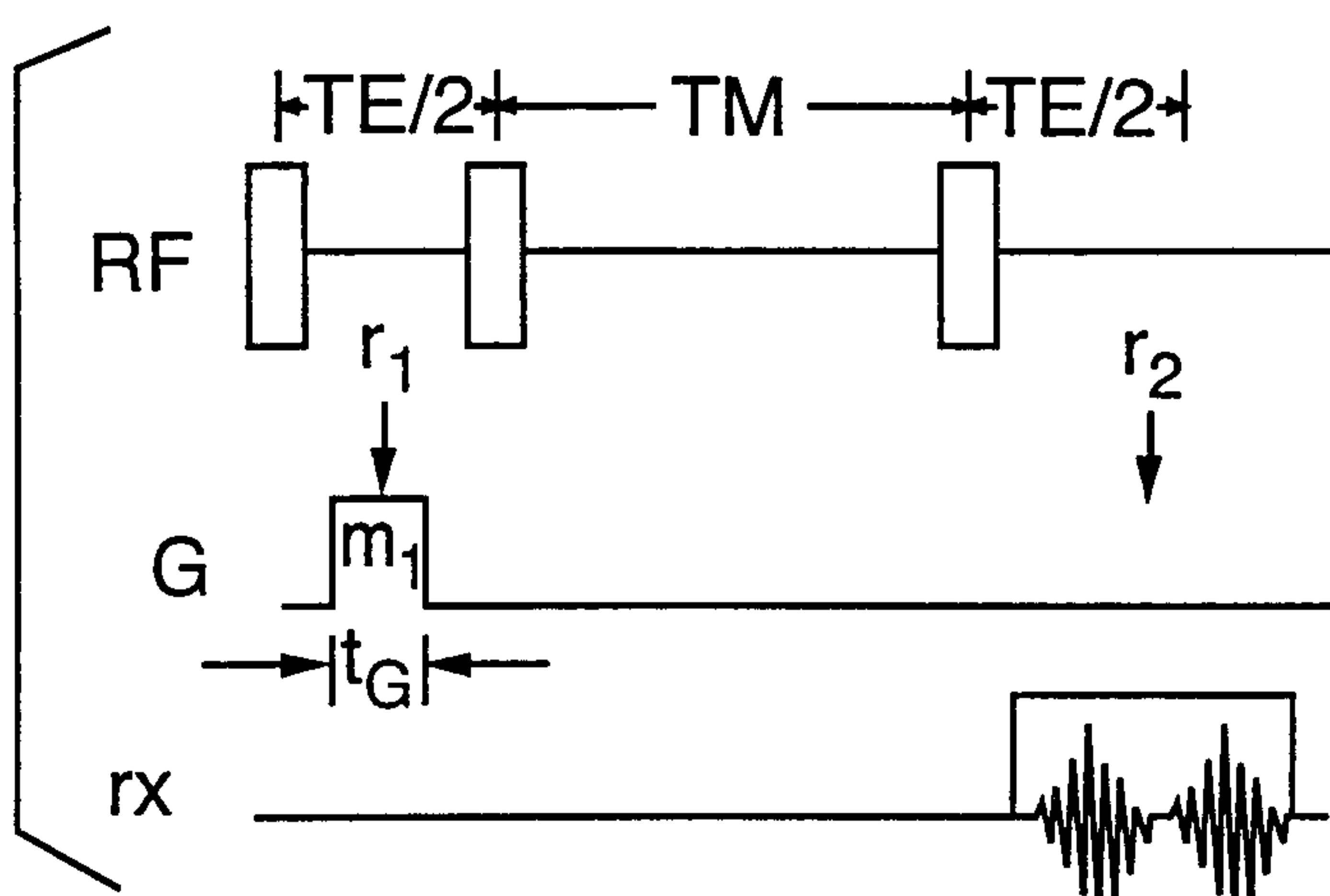


FIG. 11 B



Spin wheel after phase labeling

z pulse around the axis
of the spin wheel

The diagram illustrates a double-slit interference experiment. A horizontal line labeled 'x' on the left and 'y' on the right represents the observation screen. Two slits, labeled 'a' and 'b', are positioned on a vertical line. A phase shifter, represented by a circle with a diagonal line through it and labeled ϕ , is placed above slit 'a'. A curved arrow indicates the path of a wave from the source to the screen. The interference pattern on the screen is shown as a series of alternating bright and dark horizontal bands.

FIG. 12

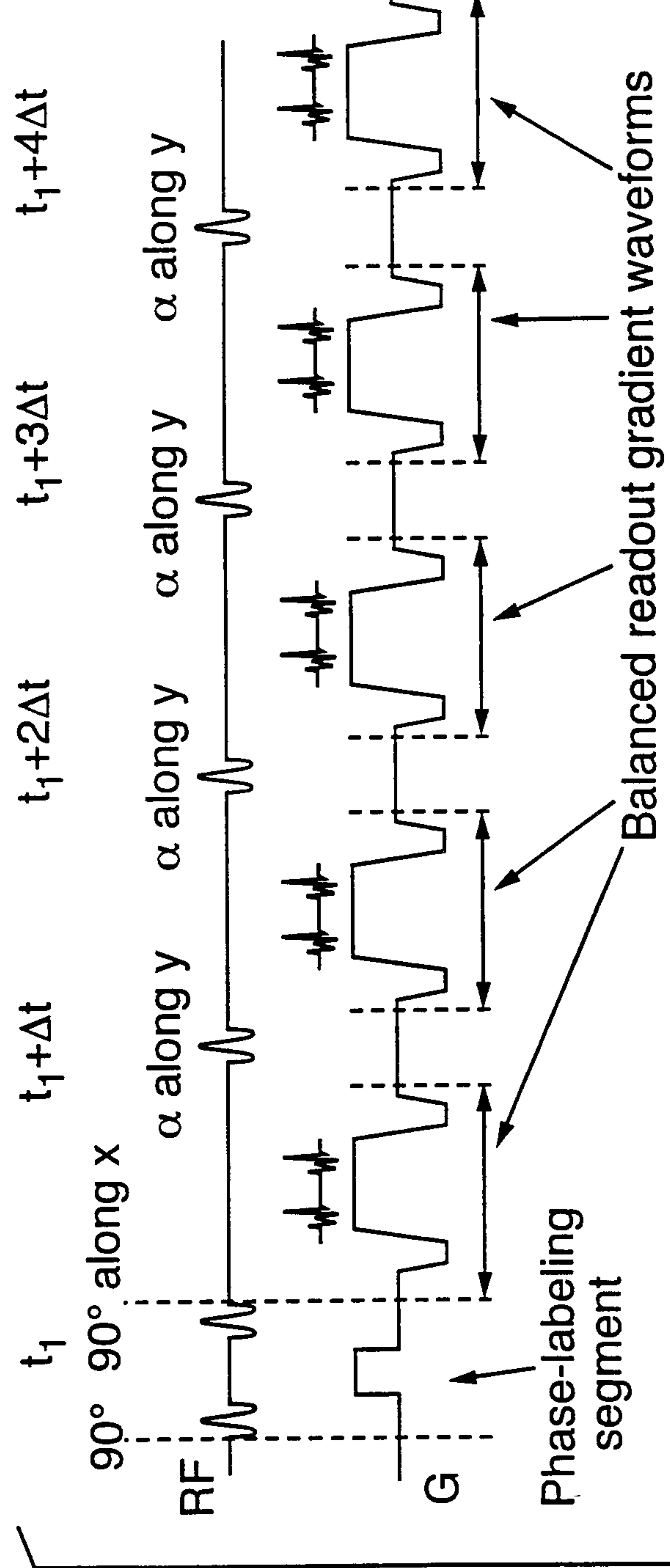
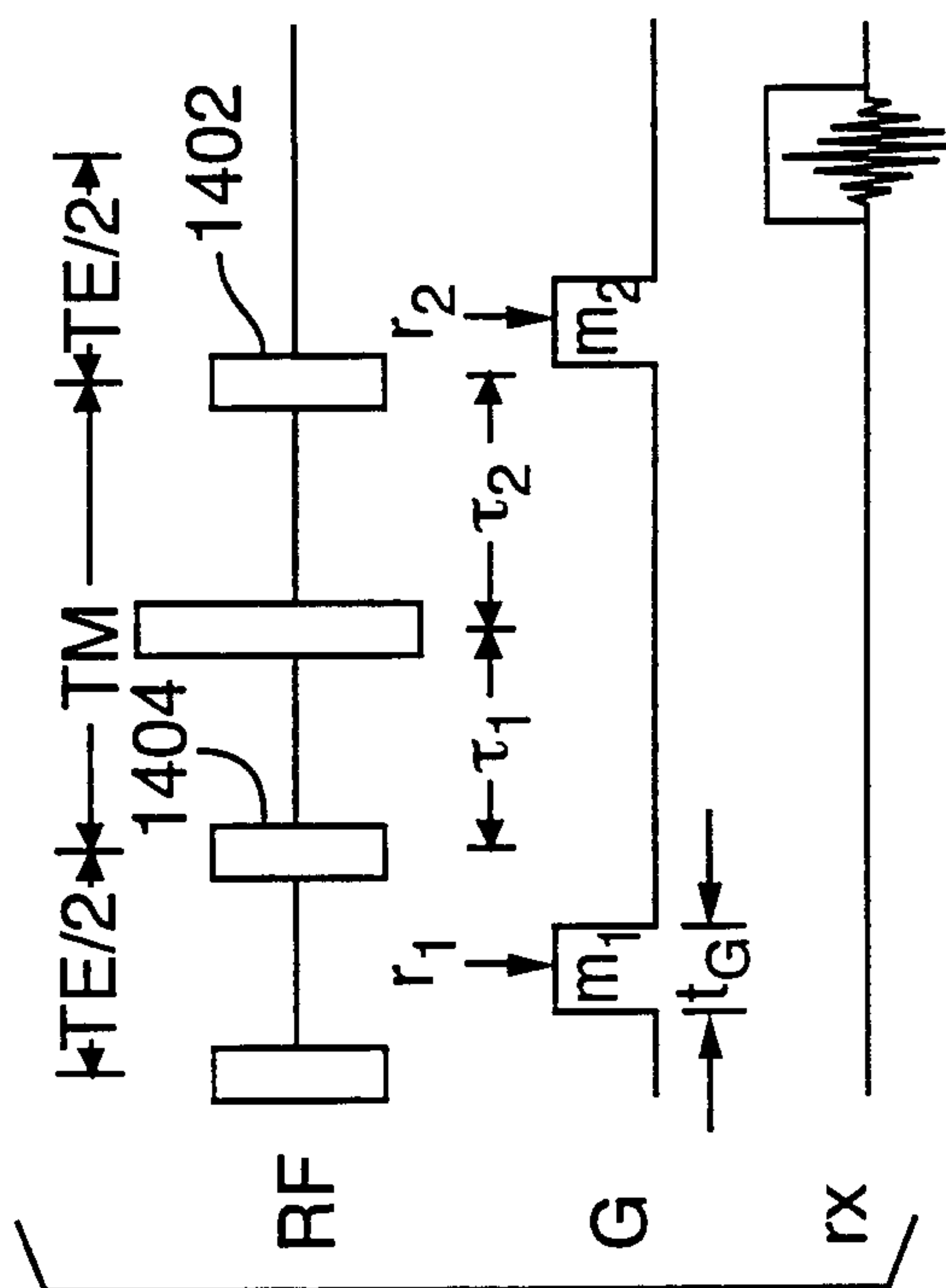


FIG. 14



Balanced slice selective RF pulse:

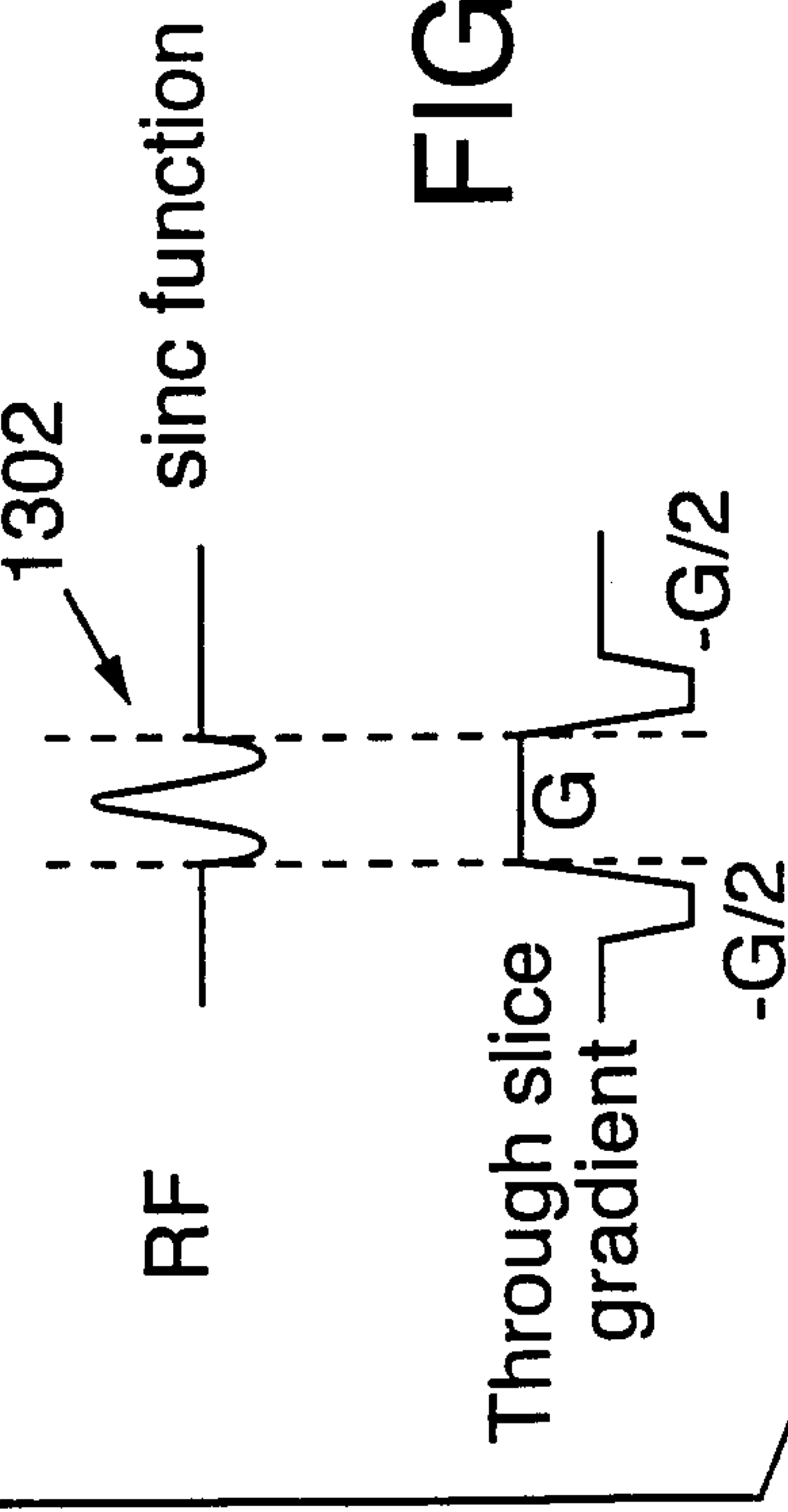


FIG. 13

